Novel Insulin Delivery Profiles for Mixed Meals in Basal-Bolus and Closed-Loop Artificial Pancreas Therapy for Type 1 Diabetes Mellitus

Asavari Srinivasan

LUND UNIVERSITY

Department of Automatic Control

Msc Thesis
ISRN LUTFD2/TFRT--5928--SE
ISSN 0280-5316

Department of Automatic Control
Lund University
Box 118
SE-221 00 LUND
Sweden

Printed in Sweden by Media-Tryck
Lund 2013

Abstract

Traditional basal-bolus and closed-loop artificial pancreas therapy for type 1 diabetes mellitus were studied in the present work and novel insulin delivery profiles have been identified.

Type 1 diabetes is a chronic condition resulting from autoimmune destruction of the pancreatic insulin producing β-cells. Inadequate insulin secretion prevents efficient glucose metabolism and is a serious health risk. Major available treatment modes are multiple daily injections of insulin and insulin pump therapy providing continuous subcutaneous infusion. General insulin regimens for low- and high-fat meals were studied *in silico* to improve current pump therapy for type 1 diabetes. This involved modifications of the FDA-accepted UVA/Padova metabolic simulation model for evaluations of meals with different absorption rates. Simulations of meals with varied fat content under this modified model demonstrated qualitative replications of published data. Subsequently, an insulin regimen library with optimized regimens under open- and closed-loop settings for a variety of meal compositions was constructed using the particle swarm optimization algorithm.

Calculations show that the optimal open-loop insulin delivery profiles for low-fat meals comprise a normal bolus or short square wave depending on the size of the meal. The preferred delivery pattern for large meals is a short insulin wave due to the increased risk for hypoglycemia. Interestingly, the optimal open-loop regimens for high-fat meals are typically biphasic, but can extend to multiple phases for large slow absorbing meals. Furthermore, individual *in silico* optimizations revealed that patients with high insulin sensitivity could benefit from biphasic insulin deliveries when consuming high-fat meals. Preliminary investigations of the optimal closed-loop regimens under varied fat content also display bi- or triphasic patterns for high-fat meals and are primarily influenced by the carbohydrate content in the meal.

The novel insulin delivery profiles identified in this work comprise new and unique waveforms that provide better control of postprandial glucose excursions than existing schemes. Furthermore, the novel regimens are also more or similarly robust to uncertainties in various parameter estimates with the closed-loop schemes displaying superior performance and robustness. The proposed closed-loop strategy does not rely on optimal basal therapy and is therefore a realistic approach that could have real-life applications in an artificial pancreas.

Keywords: type 1 diabetes, insulin pump therapy, insulin dosage, artificial pancreas, particle swarm optimization, biomedical control

Acknowledgements

I am deeply indebted to Professor Francis J. Doyle III for providing me with an opportunity to do this thesis work under his supervision and for his support throughout this work.

Helpful suggestions and encouragement received from Dr. Eyal Dassau is also gratefully acknowledged.

I would also like to thank Joon Bok Lee for his invaluable help and support. You have been an excellent mentor and I'm very grateful for all the helpful advice and interesting discussions we've had.

Working in the Doyle group has been a very pleasant and memorable experience for me and I wish to thank all my colleagues for the same.

Finally, I'm also very grateful for my family's unconditional love and support. I would never have made it without your continuous encouragement and faith in me.

Asavari

Contents

List of Symbols

AUC	Area under blood glucose response curve
APS	Artificial Pancreas System
BG	Blood glucose concentration
CHO	Carbohydrate
CFP	Carbohydrate, Fat, Protein
CSII	Continuous Subcutaneous Insulin Infusion
GI	Glycemic Index
ICR	Insulin-to-carbohydrate ratio
MDI	Multiple Daily insulin Injections
MPC	Model Predictive Control
PID	Proportional-integral-derivative control
PSO	Particle Swarm Optimization
SC	Subcutaneous glucose measurement
b, c	Model parameters for the simulated glucose absorption
c_1, c_2	Cognitive and social coefficients in the PSO algorithm
D	Amount of ingested glucose
$\delta(t)$	Discrete unit impulse function
f	Fraction of intestinal glucose absorption that appears in plasma

$H(t)$	Heaviside unit step function
K_c	Proportional controller gain
k_{21}	Rate constant of grinding in the digestion process
k_{abs}	Rate constant of intestinal glucose absorption
k_{empt}	Rate constant of gastric emptying
k_{max}	Maximum glucose absorption rate constant
k_{min}	Minimum glucose absorption rate constant
m	Amount of carbohydrates
P_g	Vector of coordinates for globally best found position
P_i	Vector of coordinates for locally best found position
$q_{gut}(t)$	Amount of glucose in intestine
$q_{sto}(t)$	Amount of glucose in stomach
$q_{sto1}(t)$	Amount of solid phase glucose in stomach
$q_{sto2}(t)$	Amount of liquid phase glucose in stomach
r_1, r_2	Coefficients in the PSO algorithm
t_F	Duration of insulin wave
τ_D	Derivative time
τ_I	Integral time
$u(t)$	Amount of insulin
u_F	Full insulin dose calculated from meal size and ICR estimates
V_i	Vector of coordinates for particle's current velocity
w	Scaling factor in the PSO algorithm
X_i	Vector of coordinates for particle's current position

1. Introduction

Diabetes mellitus is a chronic condition caused either by the inability of the pancreas to produce enough insulin or insufficient insulin secretion accompanied by the body's resistance to the effects of insulin (Daneman, 2006). The former is known as type 1 diabetes mellitus and is the focus of this thesis work. Without adequate insulin secretion, the body is unable to metabolize blood glucose and use it as an efficient energy source. Since glucose is one of the main energy sources for most cells in the body, a stable glucose concentration is essential to avoid serious complications (Stemmann, 2013). Hence, people with diabetes require insulin therapy to maintain normal blood glucose concentrations.

Rapid increases in blood glucose concentration resulting from meals are difficult to control in people with diabetes mellitus due to the lack of endogenous insulin production. As a result, meal compensation is one of the main challenges associated with blood glucose control. Type 1 diabetes mellitus is most commonly treated with subcutaneous insulin injections (Farmer et al., 2008). This is a type of open-loop insulin delivery that requires user "announcements" of meals and exercise events. A more developed form of this open-loop method is insulin pump therapy, which is a continuous insulin infusion system that delivers insulin subcutaneously. It provides basal insulin continuously throughout the day and delivers additional boluses around mealtimes based on user inputs. Automated closed-loop insulin delivery, also referred to as the artificial pancreas (AP), is an emerging treatment approach for type 1 diabetes mellitus that will ideally eliminate patient involvement in determining insulin boluses prior to meals and exercise. Several control algorithms for this approach have been proposed, the main algorithms being model predictive control (MPC) (Dassau et al., 2013), proportional-integral-derivative (PID) control (Kumareswaran et al., 2012), and fuzzy logic control (Liu et al., 2013).

This thesis aims at finding optimal insulin regimens for a variety of meal compositions using the Particle Swarm Optimization method (Kennedy et al., 1995). This is done in both an open-loop and a closed-loop setting with user announcements through *in silico* trials on ten adult subjects. The main purpose of this research is to improve open- and closed-loop insulin therapy by creating an insulin regimen optimizer that can be used to construct an insulin regimen library with a set of optimal bolus recommendations for various meal types of different sizes.

The thesis work was conducted in the research group of Professor Francis J. Doyle III at the Department of Chemical Engineering, University of California, Santa Barbara in cooperation with the Sansum Diabetes Research Institute.

1.1 Problem Statement

With conventional basal-bolus (open-loop) delivery techniques, the patient must either determine the insulin dose to be administered or provide information about an upcoming meal or exercise. The main challenge in open-loop basal-bolus meal compensation lies in choosing the appropriate insulin regimen because the postprandial blood glucose profile varies with meal composition. Since the meal absorption rate is dependent on meal composition, the insulin regimen needs to be altered between different meal types to obtain optimal blood glucose control. Choosing the wrong insulin regimen can result in postprandial hyper- or hypoglycemia, which can cause serious health problems such as ketoacidosis, cardiovascular disease, kidney failure, and blindness (WHO, 2013).

Insulin pump therapy is a commonly used open-loop method that requires the patient to estimate the meal or exercise load, after which the device determines the change in insulin infusion that is necessary to maintain near-euglycemia (Farmer et al., 2008). The traditional insulin pump offers only a limited number of bolus options, and to the author's knowledge, other insulin regimens have not yet been explored.

1.2 Objective

This thesis aims at finding the optimal insulin regimens in both open- and closed-loop settings for various meal types through *in silico* trials. It has been consistently shown that the choice of insulin regimen is crucial for good postprandial blood glucose control and is the motivation for this thesis work. The aim is to improve open- and closed-loop insulin therapy by developing an insulin regimen optimizer that can be used *in silico* for a range of different meals. With the given optimizer it will be possible to construct an insulin regimen library with a set of optimal bolus recommendations for various meal types of different sizes under both open- and closed-loop insulin therapies based on each subject's individual clinical parameters.

1.3 Thesis Outline

The first chapter of this thesis provides an introduction to diabetes mellitus, defines the problem, and describes the objectives of this work. The following chapter provides additional background information on type 1 diabetes mellitus, blood glucose homeostasis, available treatment options and insulin regimens as well as the artificial pancreas. Subsequently, the preparatory work and analysis for enabling simulation of slow absorbing meals is presented. This is followed by an introduction to the concept of open- and closed-loop insulin regimen optimization as well as a presentation of the results for three different meal types. The results from the robustness analysis are presented next, providing a comparison with existing schemes. The final chapter presents a conclusion of the results obtained in this study and offers some suggestions for future work.

2. Background

Diabetes mellitus is classified into two main types: type 1 and type 2. Type 2 diabetes is caused by insufficient insulin secretion accompanied by insulin resistance and is the most common form of diabetes, affecting 90% of people with diabetes around the world. Conversely, type 1 diabetes is a condition characterized by the destruction of pancreatic β-cells and currently affects 10% of people with diabetes (WHO, 2013). All types of diabetes mellitus lead to chronically elevated blood glucose concentrations. This is dangerous since experiencing high blood glucose concentrations over long periods of time can lead to serious health problems such as ketoacidosis, a life-threatening condition (Williamson, 2011).

Diabetes currently affects more than 371 million people worldwide and approximately 50% remain undiagnosed (IDF, 2013). Most people with diabetes are between 40 to 59 years of age. However, the number of young people suffering from diabetes is increasing, with 78 000 children developing type 1 diabetes each year (IDF, 2012). Diabetes is currently one of the leading causes of blindness and kidney failure and is predicted to become the seventh leading cause of death in the world by 2030 (WHO, 2013).

2.1 Type 1 Diabetes Mellitus

Type 1 diabetes mellitus is a chronic condition that causes selective destruction of insulin producing pancreatic β-cells. Since these are the only cells that produce insulin in the body, this destruction causes a loss of endogenous insulin production, leading to absolute insulin deficiency. Type 1 diabetes mellitus can be further classified into type 1A and type 1B diabetes, of which the first kind results from a cell-mediated autoimmune attack on the β-cells. The mechanism for the β-cell destruction in type 1B diabetes is currently unknown, but possibly involves certain genetic markers (Daneman, 2006). Without adequate insulin secretion, the body is unable to metabolize blood glucose and use it as an efficient energy source. The body cells are thus forced to use fatty acids for fuels, causing a toxic buildup of keto acids in the body over time (Williamson, 2011).

Studies suggest that the development of type 1 diabetes depends on both environmental factors as well as a genetic predisposition to the disease (Daneman, 2006). It can develop at any age, but typically occurs in childhood or adolescence with both genders being at equal risk. Some of the risk factors for developing type 1 diabetes include: having a parent with type 1 diabetes, having other autoimmune disorders, and being ill in early infancy (Univ. of Maryland,

2013). Common symptoms associated with the disease are great thirst, hunger, weight loss, and a need to urinate often (Rubin, 2008).

Without treatment, people with type 1 diabetes experience persistently elevated blood glucose concentrations, which can lead to serious damage to the body, particularly to the nerves and blood vessels (Rubin, 2008). There are numerous health risks associated with diabetes, such as blindness, kidney failure, and extensive nerve damage (Daneman, 2006). Although there is no known cure for diabetes, the aim of diabetes treatment is to avoid such serious complications or at least slow down their development.

2.2 Blood Glucose Homeostasis

Glucose is a monosaccharide that the body receives through dietary sources or is produced primarily from carbohydrates, but also from protein and fat. It is one of the main energy sources for most cells in the body. Upon meal ingestion, glucose is transported from the intestine and absorbed directly into the blood. It is then carried through the bloodstream to provide energy to various cells in the body. (McMillin, 1990)

Glucose homeostasis is a regulatory process involving multiple pancreatic hormones: insulin, glucagon, amylin, incretin hormones, epinephrine, cortisol, and growth hormone (Aronoff et al., 2004). People that do not suffer from type 1 diabetes have a fully functioning glucose regulatory system that is driven mainly by the hormone, insulin. Fig. 1 provides a simplified illustration of the regulatory system in a healthy individual.

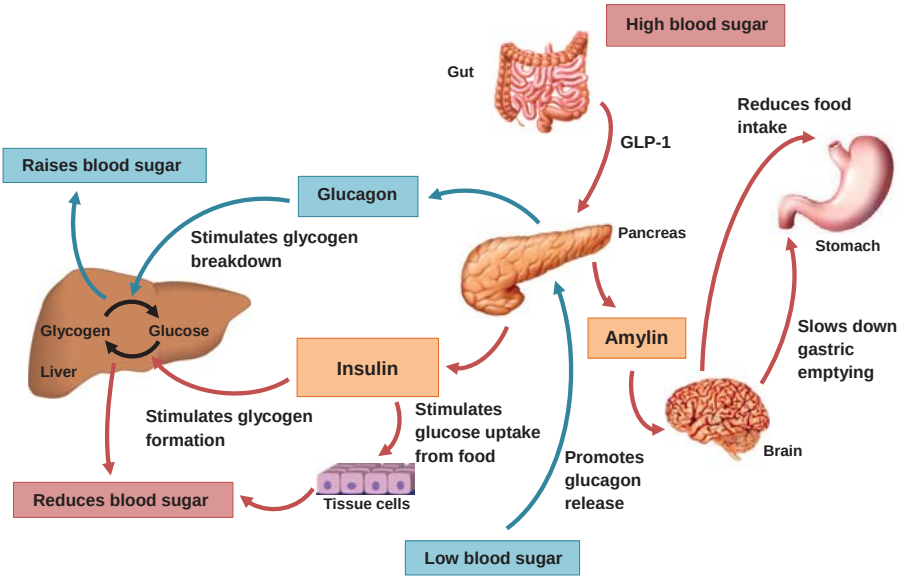

Figure 1. Blood glucose regulatory system (adapted from Marieb, 2000).

As shown in Fig. 1, insulin stimulates the rate of glucose disappearance by activating glycogen formation and glucose uptake by muscle and tissue cells. It essentially regulates the use and storage of glucose in the body, which helps maintain normal blood glucose concentrations and avoid hyperglycemia, i.e. elevated blood glucose levels (Shrayyef et al., 2010). Amylin is another glucoregulatory hormone that is co-secreted by the β-cells along with insulin to prevent postprandial spikes in blood glucose concentration. It slows down digestion and the rate of glucose entering the bloodstream (Aronoff et al., 2004). Counterregulatory hormones to insulin such as glucagon, cortisol, catecholamines, and growth hormone are released to avoid hypoglycemia, i.e. low blood glucose levels (Shrayyef et al., 2010).

Elevated blood glucose concentrations activate the glucagon-like peptide-1 (GLP-1) receptors on the β-cells. The binding of this pancreatic incretin hormone to its receptor stimulates insulin and amylin secretion and inhibits glucagon secretion by the pancreas as shown in Fig. 1. Postprandial insulin release involves an initial rapid secretion of preformed insulin followed by increased insulin production and release depending on the blood glucose concentration. Insulin secretion induces an increased glucose uptake in the cells of muscle and adipose tissue, promotes glycogenesis, and prevents glucagon secretion from the pancreatic α-cells. This signals the liver to stop glucose production by glycogenolysis and gluconeogenesis (Aronoff et al., 2004). Conversely, glucagon and epinephrine secretion are stimulated by low blood glucose

concentrations, i.e. below 65-70 mg/dl. The release of glucagon promotes the conversion of stored glycogen into glucose by binding to its receptors in the liver, while epinephrine promotes glucose production in the kidneys (Stemmann, 2013).

Inadequate insulin secretion limits the cells from accessing glucose for energy, resulting in hyperglycemia. It causes glucose to accumulate in the blood, which forces the cells to use fatty acids for fuel. However, fatty acid oxidation forms acidic ketone bodies that can result in a toxic buildup of keto acids in the body over time (Williamson, 2011). Hypoglycemia can also have serious complications such as nephropathy, retinopathy, neuropathy, and cardiovascular disease which can ultimately lead to death (WHO, 2013). Hence, a stable glucose concentration is essential to avoid serious complications.

2.3 Blood Glucose Homeostasis

In order to maintain normal blood glucose concentrations, people with type 1 diabetes require insulin therapy that supplements or replaces the body's own insulin to maintain near-euglycemia. The most common techniques are external insulin administration through multiple daily injections (MDI) and insulin pump therapy, also known as Continuous Subcutaneous Insulin Infusion (CSII) (Farmer et al., 2008).

MDI are subcutaneous injections that are administered manually using either a fine needle or an insulin pen. A slow-acting insulin analog is injected to cover the body's basal insulin needs with additional boluses of fast-acting insulin analog injected in times of high blood glucose concentrations, e.g. around mealtimes (Rubin, 2009). The alternative to MDI is insulin pump therapy, which is a continuous insulin infusion system that delivers a fast-acting insulin analog subcutaneously. It provides basal insulin continuously throughout the day and delivers additional boluses when necessary based on user input (Farmer et al., 2008). Insulin pump systems now include automated bolus calculators that can determine the amount of insulin to be delivered based on a meal size estimation provided by the user and pre-programmed settings including a personalized carbohydrate-to-insulin ratio and an insulin sensitivity factor (Zisser et al.,2010).

In addition to daily injections or pump therapy, people suffering from type 1 diabetes must maintain a healthy diet, exercise regularly, and self-monitor their blood glucose concentration throughout the day.

2.4 Traditional and Advanced Meal Compensation

The most common algorithm for determining the required insulin bolus to cover a meal is based on the estimated carbohydrate content in the meal as well as the individual insulin-to-carbohydrate ratio (ICR) determined by medical doctors. This type of insulin dose calculation is commonly referred to as carbohydrate (CHO) counting since it is based only on the carbohydrate

content (see eq. 9). A more recently developed algorithm for insulin dose calculations was presented by Pankowska et al. (Pankowska et al., 2012). It is called the CFP (Carbohydrate, Fat, Protein) algorithm and takes into account the fat and protein content in addition to the number of carbohydrates. This can be a particularly favorable calculation method for meals that contain higher percentages of fat and protein. However, CHO counting remains the most widely used algorithm for insulin bolus calculation and is presented in Eq. 1, which shows the CHO Counting Algorithm as

$$u_F = m \cdot ICR \tag{1}$$

where u_F represents the full insulin dose in units of insulin (U), m is the carbohydrate amount in grams (g), and ICR denotes the insulin-to-carbohydrate ratio.

Insulin pump systems now perform automatic calculations of the insulin dose required to cover a certain carbohydrate intake and also provide correction bolus recommendations. Examples of automated bolus calculators are the MiniMed Paradigm Bolus Wizard® [Medtronic MiniMed, Northridge, CA], Accu-Chek® Combo [Roche Insulin Delivery Systems (IDS), Inc., Fishers, IN, a member of the Roche Group], and Animas® 2020 [Animas Corp., West Chester, PA, a Johnson and Johnson company]. These devices calculate the insulin dose to be administered based on the desired blood glucose concentration, the current blood glucose concentration, a personal insulin sensitivity factor and ICR as well as an estimation of the carbohydrate amount in the meal. It has been shown that automatic bolus calculators can provide good postprandial blood glucose control without causing severe hypoglycemia. However, the performance of various automated bolus calculators can vary significantly. This is mainly because of differences in the algorithm for calculating the remaining amount of active insulin from the initial bolus, but is also due to the algorithmic rules that determine the blood glucose concentration to which a correction is made when the pump delivers a correction bolus. (Zisser et al., 2010)

The insulin regimen for a standard meal in conventional basal-bolus therapy comprises a full bolus just before the time of the meal. This type of insulin bolus can work well for certain meals, but for slower absorbing meals it is not the optimal compensation method. Recent studies suggest that insulin delivered in the form of a dual wave is the optimal compensation method for slower absorbing meals such as pizza meals (Jones et al., 2005). Other types of insulin regimens that have been considered for such meals are the traditional normal boluses and the square wave boluses. However, these regimens have not been as successful at attenuating the blood glucose concentration as the dual wave (Chase et al., 2002). The mathematical representations of the insulin profiles for a normal bolus, dual wave, and square wave are given in Eqs. 2 – 4, respectively.

$$u(t) = u_F \cdot \delta(t) \tag{2}$$

$$u(t) = \begin{cases} 0.5 \cdot u_F \cdot \delta(t), & t = 0 \\ 0.5 \cdot u_F \cdot \big(H(t - t_S) - H(t - t_F)\big), & t > 0 \end{cases} \tag{3}$$

$$u(t) = u_F \cdot \big(H(t) - H(t - t_F)\big) \tag{4}$$

where t denotes the time post-meal, u(t) is the time dependent insulin infusion in units of insulin (U), t_S signifies the start of the postprandial period, t_F corresponds to the wave duration, δ(t) is a discrete unit impulse function, and H(t) represents the Heaviside unit step function. These two discrete-time functions are defined in Eqs. 5 and 6, respectively.

$$\delta(t) = \begin{cases} 1, & t = 0 \\ 0, & t \neq 0 \end{cases} \tag{5}$$

$$H(t) = \begin{cases} 0, & t < 0 \\ 1, & t \geq 0 \end{cases} \tag{6}$$

The traditional insulin pump offers only a limited number of bolus options, as shown in Eqs. 2 – 4, with dual and square wave boluses mainly used for slow absorbing meals. To the author's knowledge, other insulin regimens have not yet been explored. Although the dual wave bolus has consistently shown better attenuation than the normal bolus, it has not been verified that this is the optimal insulin regimen for slow absorbing meals.

2.5 Artificial Pancreas

The artificial pancreas is a developing technology to help people with type 1 diabetes automatically control their blood glucose levels. It combines a glucose sensor, control algorithm, and an insulin infusion pump with the purpose of maintaining near-euglycemia through closed loop control of the blood glucose concentration (Cobelli et al., 2011). The basic structure of the artificial pancreas system (APS) is presented in Fig. 3.

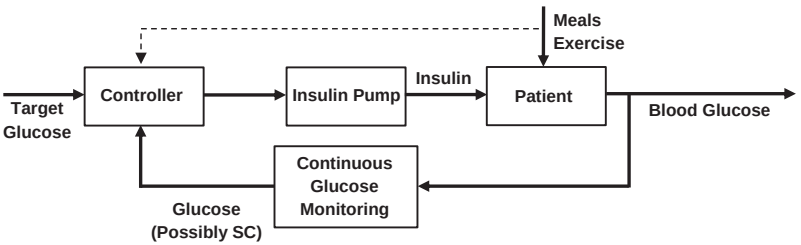

Figure 3. Block diagram of the artificial pancreas system (adapted from Doyle et al., 2007). SC denotes subcutaneous glucose measurement.

Several control algorithms for this treatment approach have been proposed, with the main algorithms being MPC, PID, and more recently fuzzy-logic control. The MPC control strategy is attractive for blood glucose control due to its applicability to systems with long time delays as well as its potential to anticipate blood glucose concentrations and handle constraints (Soru et al., 2012). Meanwhile, the PID control and fuzzy-logic algorithms have also shown promising results for applications in the APS (Kumareswaran et al., 2012; Liu et al., 2013).

An artificial pancreas has been developed by the research group at the University of California, Santa Barbara (UCSB) in cooperation with the Sansum Diabetes Research Institute. The system uses a zone-MPC control strategy in which the blood glucose concentration is controlled within a specified blood glucose concentration zone rather than at a fixed set-point (Dassau et al., 2013). Fig. 4 shows an overview of the artificial pancreas system.

Figure 4. Overview of the UCSB/Sansum Artificial Pancreas System.

3. Preparatory Analysis and Computations

The thesis work was performed using the third version of the FDA-accepted University of Virginia/Padova (UVA/Padova) metabolic simulator of blood glucose-insulin interactions (Dalla man et al., 2007; Breton et al., 2008). It facilitates simulation studies of diabetic individuals and can therefore be used in finding the optimal insulin regimen for various meal types *in silico*.

This chapter presents the preparatory analysis and describes the glucose-insulin simulation model as well as necessary model modifications that were made. In the current version of the simulator, it is only possible to simulate one meal type for which there is no straight forward way of altering the meal composition. Hence, model modifications were necessary to facilitate the simulation of slow absorbing high-fat meals.

3.1 Effects of Meal Composition

It is well known that the postprandial blood glucose profile varies significantly with meal size and composition. Meals containing large amounts of carbohydrates result in high postprandial glucose peaks. In addition, the type of carbohydrate content also influences the glucose profile. Glycemic index (GI) is used to rank how fast and high a particular food raises the blood glucose concentration compared to pure glucose. This index typically varies with the type of carbohydrates because simple carbohydrates are digested faster than complex carbohydrates. Examples of foods that are rich in simple carbohydrates are chocolate, fruit juice, and biscuits while complex carbohydrates are found in foods such as vegetables as well as whole-grain bread and cereals. A low GI is characterized by a slow glucose absorption that results in an extended blood glucose profile with a lower peak, while the opposite applies for high glycemic indices (Galgani et al., 2006). Indices assigned to meals also vary with meal composition in terms of fat and protein content. A higher percentage of fat and protein tends to slow down the rate of glucose absorption, which produces a delayed and reduced blood glucose peak compared to low-fat and low-protein meals containing the same amount of carbohydrates (Normand et al., 2004). Fig. 5 illustrates the representative differences in the glucose absorption profile between low- and high-fat meals.

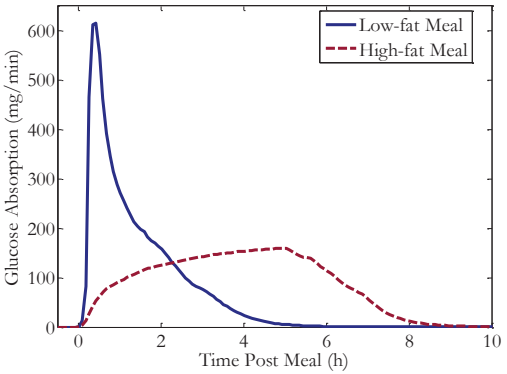

Figure 5. Simulated glucose absorption profiles for low- and high-fat meals, each containing 50 g of carbohydrates. The high-fat profile was generated *in silico* based on data from Normand et al. (2004).

3.2 Glucose-Insulin Simulation Model

The UVA/Padova metabolic simulator is based on a mathematical meal model of the glucose-insulin system developed by Dalla Man et al. (2007). It was constructed based on a data set of 204 normal individuals and models the physiological events which occur during a standard mixed meal in a person. A scheme of the glucose-insulin simulation model is presented in Fig. 6.

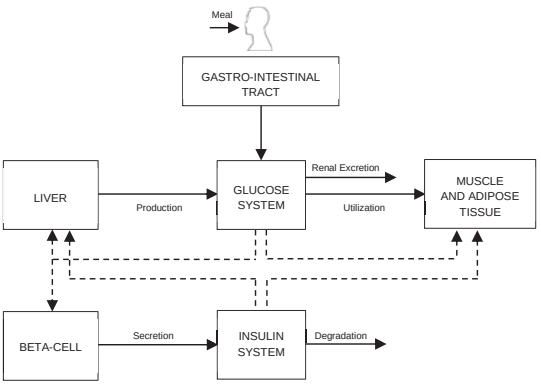

Figure 6. Glucose-insulin simulation model utilized in the UVA/Padova metabolic simulator (adapted from Dalla Man et al., 2007)

Glucose Absorption Model

The glucose absorption model is one of the sub-models of the glucose-insulin simulation model (Dalla Man et al., 2006). It is a nonlinear model describing the transit of glucose through the stomach and upper small intestine. The stomach is modeled by two compartments that represent the solid and triturated phases of the meal respectively, while the third model compartment describes the second part of the digestive tract. A scheme of the glucose absorption model is presented in Fig. 7.

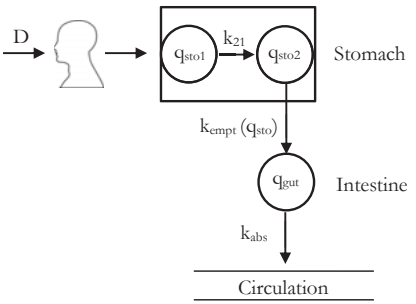

Figure 7. Glucose absorption sub-model (adapted from Dalla Man et al., 2006)

The ordinary differential equations that comprise the model are as follows (Dalla Man et al., 2006):

$$\dot{q}_{sto1}(t) = -k_{21} \cdot q_{sto1}(t) + D \cdot \delta(t) \quad (2)$$

$$\dot{q}_{sto2}(t) = -k_{empt} \cdot q_{sto2}(t) + k_{21} \cdot q_{sto1}(t) \quad (3)$$

$$\dot{q}_{gut}(t) = -k_{abs} \cdot q_{gut}(t) + k_{empt} \cdot q_{sto2}(t) \quad (4)$$

$$Ra(t) = f \cdot k_{abs} \cdot q_{gut}(t) \quad (5)$$

The variables q_{sto1} and q_{sto2} represent the amounts of solid and liquid phase glucose in the stomach, while D is the amount of ingested glucose, δ is the impulse function, q_{gut} is the mass of glucose in the intestine, k_{21} is the grinding rate, k_{abs} is the rate constant of intestinal absorption, and f represents the fraction of the absorption that appears in plasma (Dalla Man et al., 2006). The rate of gastric emptying is represented by the variable, k_{empt} and is described by a nonlinear model as shown in Eqs. 6 – 9:

$$k_{empt}(q_{sto}) = k_{min} + \frac{k_{max} - k_{min}}{2} \cdot \{\tanh[\alpha(q_{sto} - b \cdot D)] - \tanh[\beta(q_{sto} - c \cdot D)] + 2\} \quad (6)$$

$$q_{sto}(t) = q_{sto1}(t) + q_{sto2}(t) \quad (7)$$

$$\alpha = \frac{5}{2 \cdot D \cdot (1 - b)} \tag{8}$$

$$\beta = \frac{5}{2 \cdot D \cdot c} \tag{9}$$

The constants k_{min} and k_{max} represent the minimum and maximum absorption rates, respectively. The parameter b is defined as the percentage of the dose, q_{sto}, for which the rate of gastric emptying decreases at the rate $(k_{max} - k_{min}) / 2$, while the parameter c is the percentage of the dose for which the rate of gastric emptying is back to $(k_{max} - k_{min}) / 2$ (Dalla Man et al., 2006).

Simulation Model Modifications

The glucose-insulin model is represented by the Human Model Simulink block in the UVA/Padova metabolic simulator, version 3. Since the current version can only simulate one meal type, the simulation model was modified to facilitate the simulation of high-fat meals that have relatively slow absorption rates. A scheme of the modified model is presented in Fig. 8.

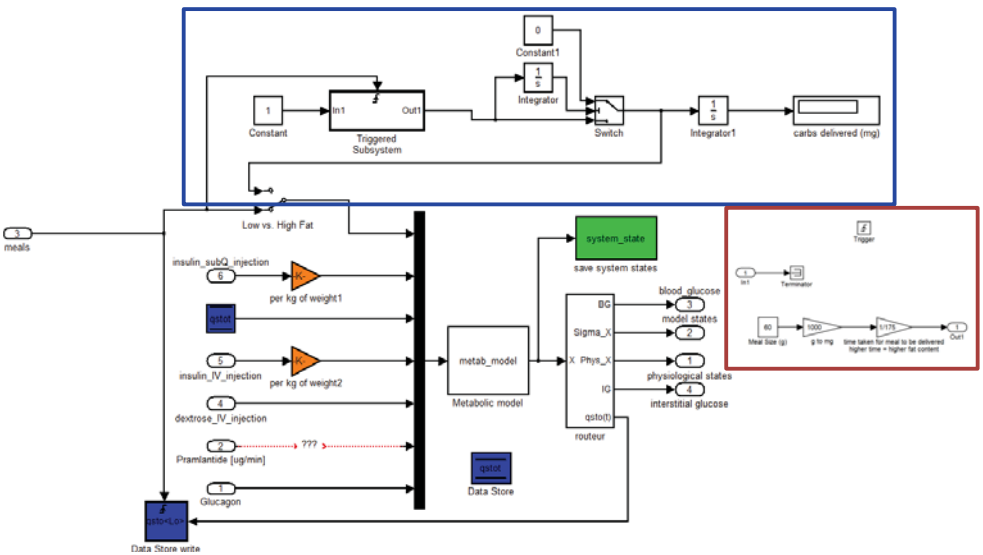

Figure 8. Modified glucose-insulin simulation model (UVA/Padova Simulator, v3)

The simulation model was modified by the addition of a loop in which an auxiliary meal delivery rate can be altered to simulate a slow absorbing meal. The additional loop is marked by

a blue rectangle in Fig. 8. The meal delivery rate is chosen depending on the absorption rate for a particular meal, where a slow meal delivery rate would be appropriate for a slow absorbing meal. The subsystem in which the meal characteristics, i.e. carbohydrate content and fictional meal delivery rate, are specified is marked by a red rectangle in Fig. 8. When the additional loop is switched on, a meal triggers the specified delivery rate until the full meal has been delivered. The switch added to the model allows an easy transition between simulation of low-and high-fat meals.

3.3 *In Silico* Replication of Published Data

To ensure realistic simulation data, the auxiliary meal delivery rate was tuned to produce a good qualitative replication of postprandial blood glucose profiles in the literature. The simulated profiles for the two high-fat meals studied were generated under similar conditions as the published data considering the time of the postprandial peak as the criterion for a good match. Specifically, the average blood glucose profiles from ten adult *in silico* subjects were compared with published data from Jones et al. (2005) and Normand et al. (2004) under this criterion.

Jones et al. conducted a study on 26 adults with type 1 diabetes to determine the optimal insulin regimen for a pizza meal. On three separate occasions, the subjects were asked to consume three pizza slices consisting of approximately 90 g of carbohydrate, 42 g of fat, 45 g of protein, 6 g of fiber, and 6 g of sugar in total. Insulin was delivered as a normal bolus, a 4 or 8-hour dual wave. They concluded that the 8 hour dual wave was the optimal insulin regimen for a pizza meal.

Normand et al. performed a study on 9 healthy women to determine the influence of dietary fat on postprandial glucose metabolism. One meal consisting of 75 g of pasta with a fat content of 55% was chosen from this study for *in silico* evaluation. Herrero et al. identified certain meal model parameters for this particular meal through constrained optimization using the MATLAB routine fmincon (Herrero et al., 2007). These parameter values were implemented in the UVA/Padova metabolic model to obtain the glucose absorption profile for a high-fat pasta meal *in silico*. The scenario was simulated under subject specific optimal basal insulin therapy and appeared a realistic estimate of the glucose absorption profile for a high-fat meal when compared to clinical data from the type 1 diabetes study conducted by Jones et al. (2004). This particular blood glucose profile will hereafter be referred to as the reference profile. As mentioned previously, the optimized model parameter values could not be used when simulating regular open- or closed-loop insulin therapy as it resulted in unrealistic blood glucose dynamics when administering insulin in addition to the basal insulin rate. Hence, the optimized parameters were only used to obtain a simulated reference profile under basal insulin therapy. This profile was then used to generate a glucose absorption profile for a high-fat pasta meal by altering the auxiliary meal delivery rate in the modified metabolic simulator (see Chap. 3.2, section: Simulation Model Modifications), as shown in Fig. 9b.

Both the pizza and pasta meals were simulated *in silico* and were programmed as 90 g and 63.4 g carbohydrate meals, respectively. These amounts are based on published data from Jones et al. (2005) and Normand et al. (2004). The modified glucose-insulin simulation model was then programmed to deliver the meals at slower rates to match the given data. Altering the auxiliary meal delivery rate made it possible to replicate the time of the peak, but since the delivery rate does not affect the magnitude of the postprandial glucose excursion, the height of the blood glucose peak could not be adjusted. The peak height for the simulated pizza meal conforms to published data and hence did not require adjustment, but there remains a quantitative mismatch for the high-fat pasta meal due to the inability to adjust the postprandial peak height. However, in connection with the insulin regimen optimization, the time of the peak is of greater interest than the peak height since this will determine the optimal timing for all insulin deliveries. After fine-tuning the auxiliary meal delivery rates, it was possible to qualitatively replicate the reference profiles, as shown in Fig. 9.

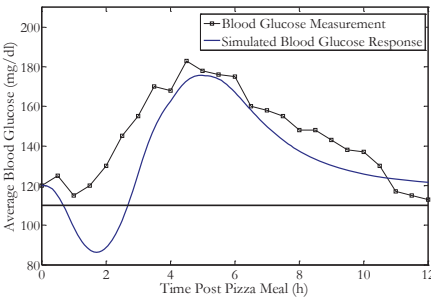

Figure 9a. Comparison of simulated ten subject average blood glucose response to a 90 g CHO pizza meal and published data from Jones et al. given a full insulin bolus at the time of the meal (Jones et al., 2005)

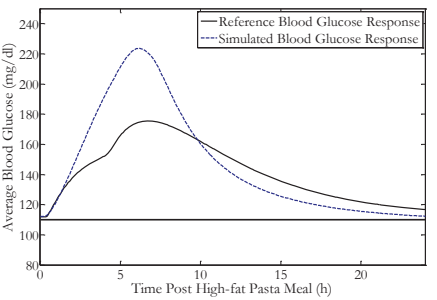

Figure 9b. Comparison of simulated ten subject average blood glucose response profiles for a 63.4 g CHO high-fat pasta meal and a simulated reference profile based on *in silico* data from Herrero et al. (2007). The scenarios were simulated under basal insulin therapy only.

Since the meal delivery rates vary with the size of the meal, the obtained values for both meal types were translated into auxiliary meal durations that are independent of meal size. The durations for the pizza and high-fat pasta meals were determined to be 175 and 300 minutes, respectively. With constant meal durations it is thus possible to simulate these two meal types for varying amounts of carbohydrates.

Fig. 10 illustrates the scope of this thesis work, i.e. the different meal types that were studied. The figure presents the ten subject average blood glucose absorption profiles for the three different meal types of similar size: a low-fat meal, pizza meal, and high-fat pasta meal.

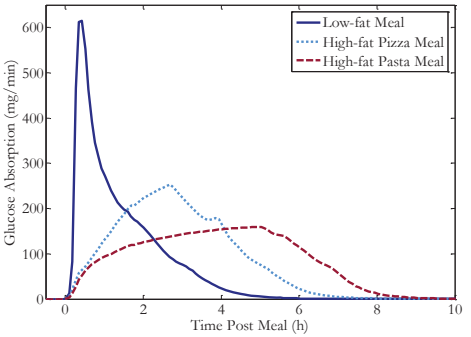

Figure 10. Ten subject average glucose absorption profiles for three different meal types, each containing 50 g of carbohydrates.

The simulated profiles shown in Fig. 10 clearly show the significant variations in glucose absorption with meal composition, with the high-fat pasta meal having the slowest absorption rate due to its high fat content. Table 1 presents certain parameters, such as area under the curve (AUC), blood glucose peak, and time of peak for the simulation of these three meal types under simple basal insulin therapy to demonstrate the effect of increased fat content on glucose absorption. These parameters are commonly used in combination with other metrics to measure controller performance and evaluate open-loop control systems for diabetes treatment. The area under the curve (AUC) is a measure of the deviation from the baseline and was calculated with a baseline of 110 mg/dl (mid-euglycemic range). It was then normalized through division by the simulation time and can thus easily be compared between simulations independent of simulation time.

Table 1. Comparison of a low-fat meal, pizza meal, and high-fat pasta meal. The presented values are averaged over ten *in silico* subjects.

Meal Type	Mean Blood Glucose Peak (mg/dl)	Time of Peak (minutes post meal)	Normalized AUC (mg/dl)
Low-fat	234.8 ± 38.9	2.6 ± 0.6	33.5 ± 17.0
Pizza	226.2 ± 38.7	4.6 ± 0.6	33.3 ± 16.8
High-fat Pasta	214.2 ± 37.9	6.4 ± 0.5	33.1 ± 16.1

Both the blood glucose peak and the time of peak vary significantly between the three meal types as shown in table 1. An increased fat percentage slows down the rate of glucose absorption which causes a delayed and reduced blood glucose peak for high-fat meals. As expected, the difference in normalized AUC between the three meals is negligible since they contain the same amount of carbohydrates. The ability to simulate both low- and high-fat meals in the modified metabolic simulator was then used to find the optimal insulin regimens for these three meal types.

4. Meal Compensation

Meal compensation is one of the biggest challenges in blood glucose control due to the variations in glucose response with different meal compositions as well as the difficulties in estimating the exact carbohydrate content in meals consumed. Since different meals produce diverse glucose absorption profiles, it is not optimal to compensate for all meals using the same insulin delivery regimen. It has been consistently reported that administering a normal bolus is not optimal for high-fat meals due to the slow rise in blood glucose (Chase et al., 2002; Jones et al., 2005). It is very important to consider this absorption delay when designing an insulin regimen for meals of this type, and many recent studies have aimed at determining the optimal insulin regimen for high-fat meals to address this issue (Chase et al., 2002; Jones et al., 2005; Scaramuzza et al., 2007).

4.1 Novel Open-loop Insulin Regimens for Low and High-fat Meals

The motivation for exploring novel insulin regimens is to improve postprandial blood glucose control in people with type 1 diabetes. Since the meal absorption rate depends on meal composition, the insulin regimen should be altered between the different meal types to obtain optimal blood glucose control. Administering a normal bolus for a high-fat meal increases the risk of postprandial hypoglycemia because the meal absorption is slower than the insulin absorption and action. *In silico* testing of various insulin regimens revealed that both open- and closed-loop blood glucose control following high-fat meals could be enhanced by an insulin regimen consisting of multiple deliveries in the form of insulin waves.

The insulin regimen for a given meal type was formulated as an optimization problem and is explained in further detail in Appendix A. Each meal scenario problem was solved using the UVA/Padova metabolic simulator, taking into account ten adult *in silico* subjects. Three different meal types were considered for the insulin regimen optimization: a standard low-fat meal, a pizza meal, and a high-fat pasta meal. Each of these was simulated as 50 g, 75 g, and 100 g carbohydrate meals, providing a total of nine different scenarios. The standard low-fat meal is the default meal type in the metabolic simulator, while the simulated pizza and pasta meals are based on published data. The aim of creating an insulin regimen optimizer is to provide a way of giving appropriate insulin bolus recommendations to patients for various meal types.

Insulin Regimen Optimization

The Particle Swarm Optimization (PSO) methodology was first introduced by James Kennedy and Russell C. Eberhart in 1995. It is a biologically inspired algorithm that has been proven efficient in solving optimization problems. PSO is a population based algorithm in which a set of potential solutions are improved iteratively based on the given cost function that is to be minimized. Each member (particle) of the population is a potential solution and is initialized with a velocity and position in the parameter space. During the optimization, the particles are moved around in the D-dimensional search space where D is the number of optimization variables. The aim is to progressively move the entire particle population to the optimal solution, i.e. the optimal combination of the optimization variables (Kennedy et al., 1995). Fig. 11 presents the basic concept of the PSO algorithm.

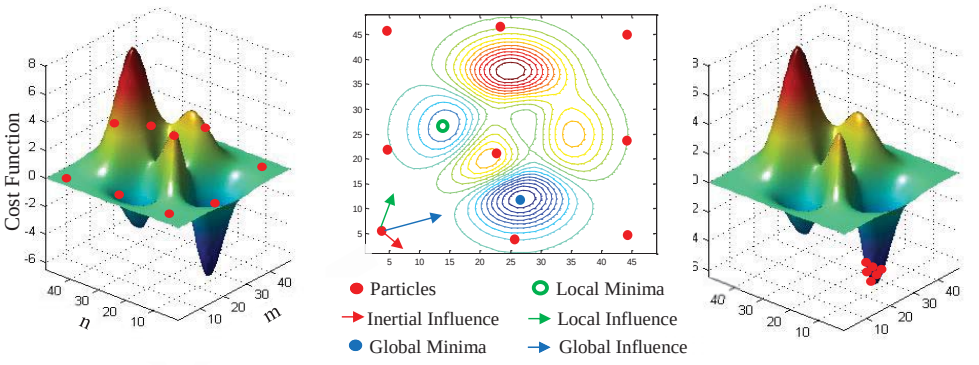

Figure 11. The basic concept of the Particle Swarm Optimization algorithm

Fig. 11 presents the basic PSO algorithm applied to a two variable optimization problem by illustrating the movement of candidate solutions (particles) in the search space. Each particle in Fig. 11 represents a particular combination of the two optimization variables, n and m, and are uniformly distributed over the search space. In the PSO algorithm, each particle is described by four vectors in the D-dimensional space: its current position $X_i = (x_{i1}, x_{i2}, \ldots, x_{iD})$, its velocity $V_i = (v_{i1}, v_{i2}, \ldots, v_{iD})$, its currently best found position $P_i = (p_{i1}, p_{i2}, \ldots, p_{iD})$, and the currently best position searched by the whole particle swarm $P_g = (p_{g1}, p_{g2}, \ldots, p_{gD})$. Each particle's position is updated iteratively as shown in Eqs. 10 – 11 (Kennedy et al., 1995):

$$V_i^{t+1} = w \cdot V_i^t + c_1 r_1 \cdot \left(P_i^t - X_i^t\right) + c_2 r_2 \cdot \left(P_g^t - X_i^t\right) \tag{10}$$

$$X_i^{t+1} = X_i^t + V_i^{t+1} \tag{11}$$

where in Eq. 10, w is a scaling factor that determines the influence of the previous velocity on the updated one. The constants c_1 and c_2 are cognitive and social coefficients, respectively and

determine the local and global influence on the updated velocity. The parameters r_1 and r_2 are random numbers that are generated from a uniform distribution in the interval [0,1]. (Kennedy et al., 1995)

The algorithm evaluates each particle's position according to the given cost function and updates the particle's best found position if the current position is better than any previous position it had. Thereafter, the best found position so far is determined based on all particles' previous best positions. The algorithm then goes on to update each particle's velocity, which is influenced by the particle's inertia, its best position, and the global best position as shown in Fig. 11 and Eq. 10. The influence of these three variables is determined by the weighting parameters w, c_1, and c_2. Given the updated velocities, each particle's position can be updated according to Eq. 11, after which all particles are moved to their new positions. The objective is to progressively move the entire population closer to the optimal solution and eventually arrive at the optimal combination of the optimization variables as shown in the right hand side of Fig. 11.

In this study, the PSO algorithm was implemented to find the optimal open-loop insulin regimens for three different meal types. It was also used to find the optimal insulin regimen under a closed-loop setting with a PID controller for which the controller parameters were also optimized using the same methodology (see Chap. 4.2 Novel Closed-loop Insulin Regimens for Low- and High-fat Meals). For both the open- as well as closed-loop cases, the insulin regimen optimization problem was designed as a multiple delivery scheme with four possible deliveries. However, the bounds for each delivery were chosen so that the deliveries are made only if it is optimal (see Appendix A). The three chosen optimization variables for each delivery are: the time of the insulin delivery, the fraction of the full insulin dose to be delivered, and the time duration of each delivery, resulting in a total of 12 variables for the given problem. The computational parameters, including constraints as well as upper and lower limits are presented in Appendix A.

Open-loop Regimens for Low-fat Meals

General optimal insulin regimens (GOR) for ten *in silico* subjects given low-fat meals comprising 50, 75, and 100 g of carbohydrates were determined using PSO. The optimization result for a low-fat meal containing 100 g of carbohydrates is presented in Fig. 12 and the results for 50 and 75 g low-fat meals in Appendix B.

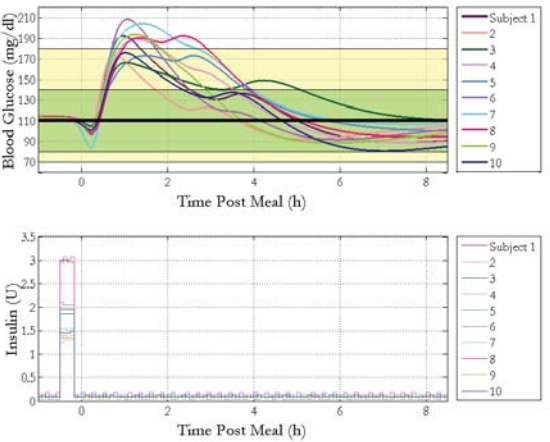

Figure 12. General optimal open-loop insulin regimen for a low-fat meal comprising100 g of carbohydrates. The upper plot shows the postprandial blood glucose response profiles for ten *in silico* subjects, and the bottom plot presents the optimal insulin delivery pattern for all ten subjects. The optimized insulin delivery regimen maintains a majority of the subjects within the 70-180 mg/dl safe zone throughout the trial despite the high carbohydrate content of the meal.

The results in Fig. 12 show that the optimal insulin regimen for a low-fat meal comprising 100 g of carbohydrates is a 15 minute wave delivered 30 minutes prior to the meal. However, the optimal insulin regimen for a 50 and 75 g carbohydrate low-fat meal is a normal bolus delivered 30 minutes before the meal (see Appendix B). Although early insulin administration is theoretically optimal, it is important to consider the potential risks of hypoglycemia if the meal is delayed. Theoretically, the results are feasible considering the increased risk of hypoglycemia that follows a normal bolus when compensating for larger meals. However, it is important to note that these results were obtained because the earliest possible insulin delivery was constrained to 30 minutes prior to the meal due to the practical difficulties of meal planning. Since the meal is large and fast absorbing, it is difficult to maintain the blood glucose concentrations for all ten subjects within the safe range of 70 – 180 mg/dl, as shown in Fig. 12. The results for all three meal sizes suggest that insulin should be administered at least 30 minutes

before the start of the meal for low-fat meals of significant size. This is explained further by the simulated intestinal glucose absorption profiles for this meal type in Fig. 13.

.

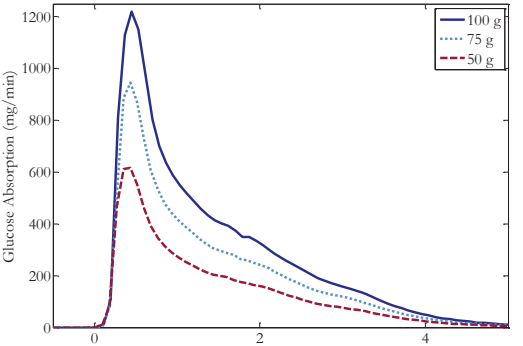

Figure 13. Ten subject average intestinal glucose absorption profile for low-fat meals comprising 50, 75, and 100 g of carbohydrates.

The fast digestion of low-fat meals causes a rapid glucose absorption, as shown in Fig. 13. The glucose absorption peaks occur approximately 30 minutes after the start of the meal. The absorption of glucose is relatively fast compared to the time needed for insulin absorption and action since insulin is delivered subcutaneously as per current technology. It is therefore necessary to administer the insulin prior to the meal to avoid severe hyperglycemia, as proposed by the general regimen presented in Fig. 12.

Optimal regimens for each individual subject were also determined to confirm that the general regimen is feasible, and to find potential trends that may be used as guidelines when prescribing regimens to certain groups of patients. The individually optimized regimens (IOR) for a 100 g low-fat meal are shown in Fig. 14.

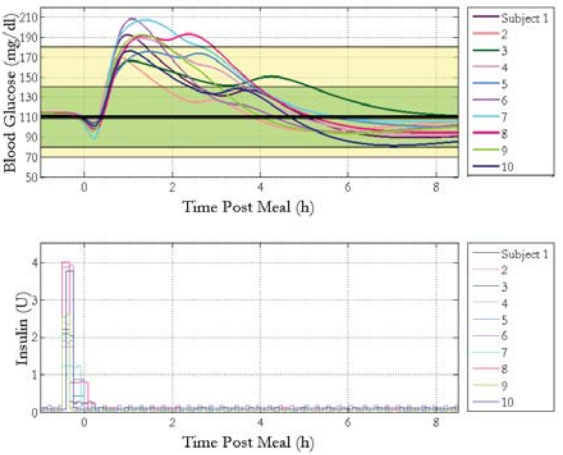

Figure 14. Individual optimal open-loop insulin regimens for a low-fat meal comprising 100 g of carbohydrates. The upper plot shows the postprandial blood glucose profiles for ten *in silico* subjects, and the bottom plot presents the individual optimal insulin delivery patterns for all ten subjects.

As shown in Fig. 14, although a few subjects display an extended wave pattern, most of the individual regimens comprise one short square wave. These results validate the general regimen since all individual insulin profiles are very similar to the general optimal regimen in Fig. 12. Fig. 15 presents the individual regimens on a normalized scale and compares the average insulin profile to the general optimal regimen.

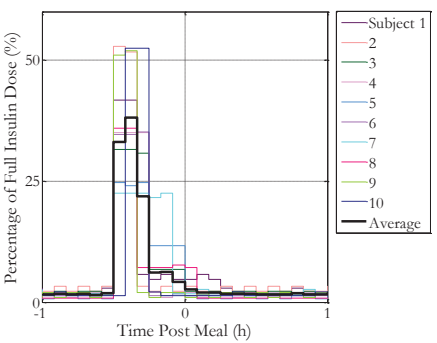

Figure 15a. The optimized individual insulin delivery patterns for ten *in silico* subjects and the average insulin profile based on the individual patterns given a low-fat meal comprising 100 g of carbohydrates.

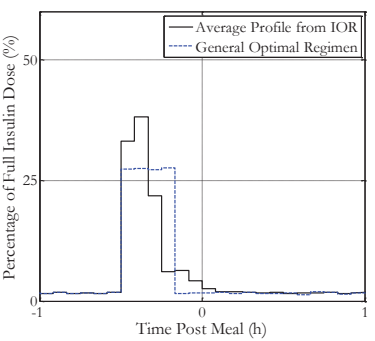

Figure 15b. Comparison between the average insulin profile based on individually optimized regimens and the general regimen optimized for ten *in silico* subjects given a low-fat meal comprising 100 g of carbohydrates.

The similarities between the general regimen and the average insulin profile indicate that providing a general recommendation to patients can be reasonable for this meal type. However, there are slight variations between the individual regimens, as shown in Fig. 16, which compares two distinguishable wave patterns.

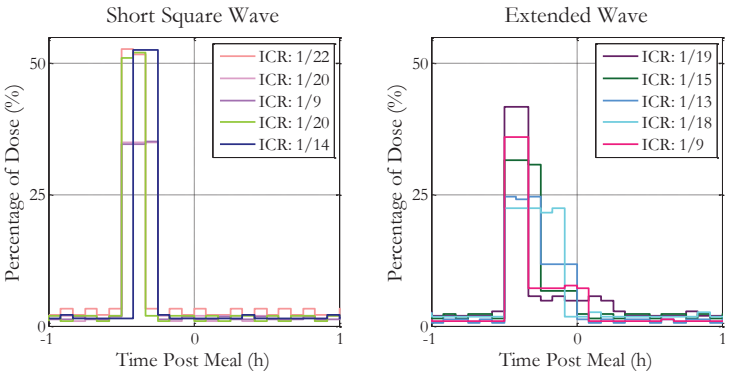

Figure 16. Observed trends in insulin profiles for ten *in silico* subjects. The left plot shows the group of *in silico* subjects whose optimal insulin delivery regimen comprises one short square wave, and the right plot presents the group of subjects whose individual regimens have an extended wave pattern. ICR denotes the insulin-to-carbohydrate ratio and is a measure of insulin sensitivity.

The results in Fig. 16 show that 50% of the subjects have optimized individual regimens comprising a short square wave, while the others have an extended wave pattern. Although the exact reason for these profile variations could not be linked to the ICR, the results are not unrealistic as other biological effects such as the insulin absorption rate, fitness, and others may also play a role in a subject's blood glucose response. Interestingly, there appears to be a small but consistent trend for highly sensitive subjects (low ICR), since they all have short square wave profiles, as shown in the left hand side of Fig. 16. This indicates that subjects with high insulin sensitivities may benefit further from a slower infusion rate due to the relatively faster insulin action in these subjects.

To confirm the optimality of the obtained results, the performance of the general and individual regimens is compared to that of a normal bolus delivered 30 minutes prior to the meal in Fig. 17.

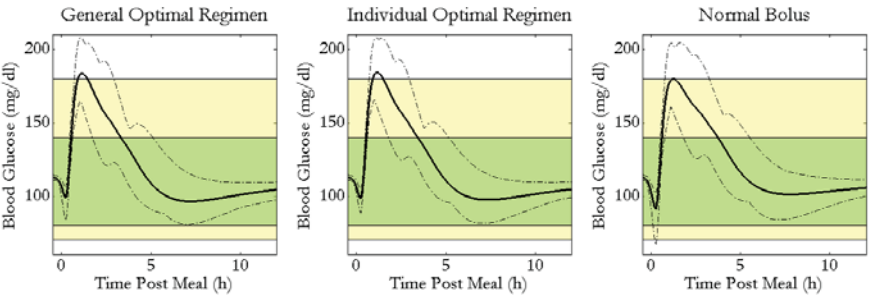

Figure 17. Comparison of the optimal regimens and a normal bolus delivered 30 minutes prior to a low-fat meal comprising 100 g of carbohydrates. The solid curves represent the average blood glucose profiles for ten *in silico* subjects and the area between the dashed lines shows the range of variability.

Fig. 17 shows that the performance of the three insulin regimens is almost indistinguishable since they all produce similar average blood glucose profiles and ranges of variability. For a fast absorbing low-fat meal there are only a limited number of insulin regimens that will provide good blood glucose control, which is why the results for the various regimens are similar. This is also confirmed by the data in Table 2, which provides a comparison of the regimens by a set of performance metrics, averaged over ten *in silico* subjects.

Table 2. Comparison of three insulin regimens for a low-fat 100 g carbohydrate meal.

Insulin Regimen	**Normalized AUC (mg/dl)**	**Mean % Time within 70-180 mg/dl**	**Mean % Time within 80-140 mg/dl**	**Mean Blood Glucose Peak (mg/dl)**
General Regimen	9.9 ± 2.1	97.6 ± 2.5	91.4 ± 3.1	186.8 ± 13.9
Individual Regimen	9.8 ± 2.1	97.6 ± 2.5	91.2 ± 3.0	186.9 ± 14.6
Normal Bolus 30 Minutes Prior to Meal	9.8 ± 2.2	97.5 ± 2.8	90.3 ± 3.4	185.0 ± 14.7

Although the results in Table 2 show similar performance for all three regimens, it is important to note that the general and individual optimal regimens show lower standard deviation for all measured parameters and can maintain blood glucose concentrations within the

euglycemic range marginally longer than the normal bolus. A statistical paired t-test with an α-level of 0.05 confirms that the normal bolus regimen is close to optimal since it shows that the optimal general regimen is significantly better only in terms of the percentage of time spent in euglycemia. Furthermore, a paired t-test comparing the general and individual regimens revealed that the individually optimized regimens are not significantly better, suggesting that a general recommendation can be used for this meal type.

Observations of the overall results for low-fat meals (100, 75, and 50 g carbohydrate content) suggest that meals of significant size should be announced at least 30 minutes prior to the meal for optimal blood glucose control. The best meal compensation is achieved by a normal bolus or a short square wave depending on the size of the meal.

Open-loop Regimens for High-fat Pizza Meals

Next, the generalized optimal insulin regimens for high-fat pizza meals of various sizes were found using PSO. Results for meals containing 50 and 75 g of carbohydrates are presented in Appendix B, and the result for a 100 g pizza meal is shown in Fig. 18.

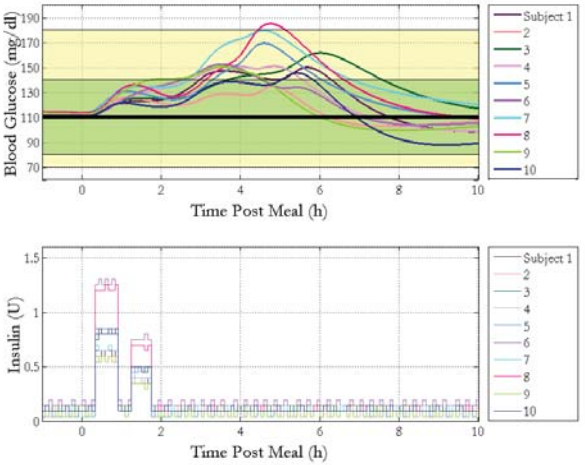

Figure 18. Optimal open-loop insulin regimen for a high-fat pizza meal containing 100 g of carbohydrates. The upper plot shows the postprandial blood glucose profiles for ten *in silico* subjects, and the bottom plot presents the optimal insulin delivery pattern for all ten subjects. The optimized insulin delivery regimen maintains safe blood glucose concentrations for all subjects throughout the trial despite the high carbohydrate content of the meal

The results in Fig. 18 show that the general optimal insulin regimen for a large pizza meal comprises two consecutive square waves of similar lengths. This biphasic regimen maintains the

blood glucose concentration within the range of 70 – 180 mg/dl for most subjects and results in only one mild hyperglycemic event. The general regimen for a 75 g pizza meal is similar to that for the 100 g meal presented in Fig. 18. However, the result obtained for a 50 g meal suggests that a long square wave provides better compensation for smaller meal sizes (see Appendix B). The slower insulin delivery in the form of a single wave can be explained by the relatively slow blood glucose excursion for smaller meals of this type, as illustrated by the simulated glucose absorption profiles in Fig. 19.

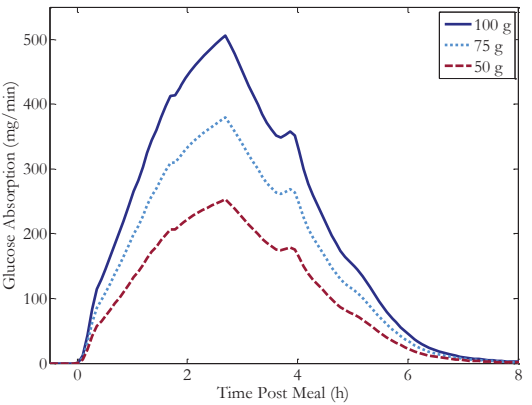

Figure 19. Ten subject average intestinal glucose absorption profiles for high-fat pizza meals comprising 50, 75, and 100 g of carbohydrates.

High-fat meals such as pizza meals generally exhibit slow glucose absorption as a result of the longer digestion process. The absorption peaks for these particular pizza meals occur approximately 2 hours and 40 minutes after the start of the meal. The glucose absorption is relatively slow compared to the time needed for insulin absorption and action, which is why the general optimal regimen does not suggest insulin delivery prior to the meal. Insulin administration that is too early could potentially result in hypoglycemia because of the slow digestion. The optimization results for all three pizza meals propose regimens in which the insulin deliveries are made within the first two hours after the start of the meal. The time of the glucose absorption peak is similar for all three meal sizes and is what determines this specific time period for insulin deliveries. As mentioned previously, the results suggest that biphasic regimens are more favorable when consuming larger meals. This is feasible since larger meals cause a faster rise in glucose concentration compared to smaller meals, as indicated by the glucose absorption profiles in Fig. 19.

Individual optimal regimens were also determined for each of the ten subjects to examine potential trends that might be useful in prescribing insulin regimens to patients. The individual optimal insulin regimens for a 100 g high-fat pizza meal are shown in Fig. 20.

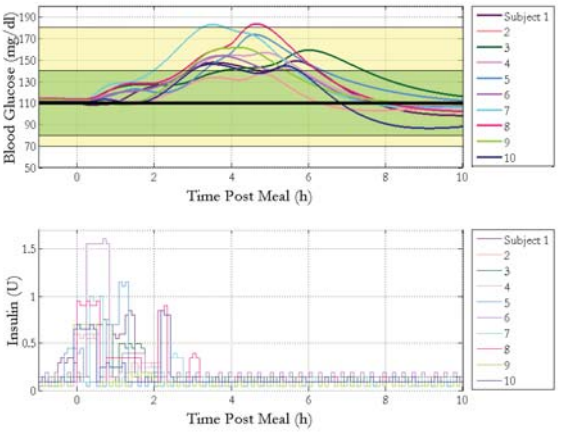

Figure 20. Individual optimal open-loop insulin regimens for a high-fat pizza meal comprising 100 g of carbohydrates. The upper plot shows the postprandial blood glucose profiles for ten *in silico* subjects, and the bottom plot presents the individual optimal insulin delivery patterns for all ten subjects.

Most of the individual regimens display biphasic patterns that are similar to the general optimal regimen. Although some subjects have multiphasic regimens, the biphasic pattern is the most common among the individual regimens. This implies that the general regimen in Fig. 14 conforms to the results from the individual optimizations. With the general regimen, insulin is delivered within the first two hours of the meal, following the same trend as most of the individual insulin regimens in Fig. 20. Fig. 21 presents the various individual regimens and compares the average insulin profile to the general optimal regimen.

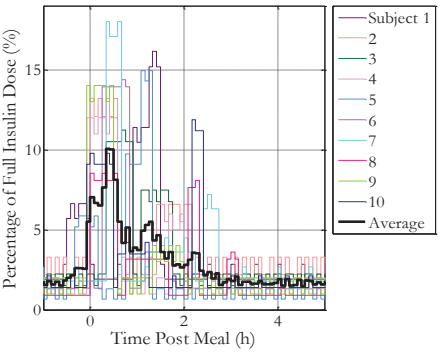

Figure 21a. The optimized individual delivery patterns for ten *in silico* subjects and the average insulin profile based on the ten individual patterns given a pizza meal comprising 100 g of carbohydrates.

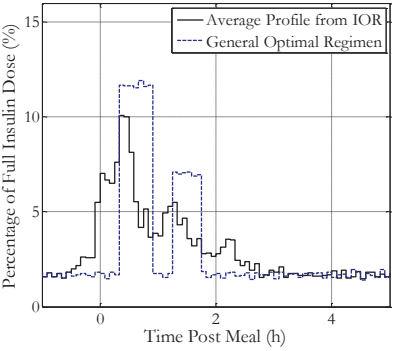

Figure 21b. Comparison between the average insulin profile based on individually optimized regimens (IOR) and the general regimen optimized for ten *in silico* subjects.

The insulin deliveries in the general regimen occur approximately at the same time as the peaks of the average insulin profile, which indicates that the regimen is a reasonable recommendation for this meal type. However, there are significant variations between the individual regimens as a result of various factors, making it difficult to recognize clear trends. One of the main factors determining the insulin regimens appears to be the ICR. Fig. 22 illustrates the various trends that can be observed between different groups of subjects.

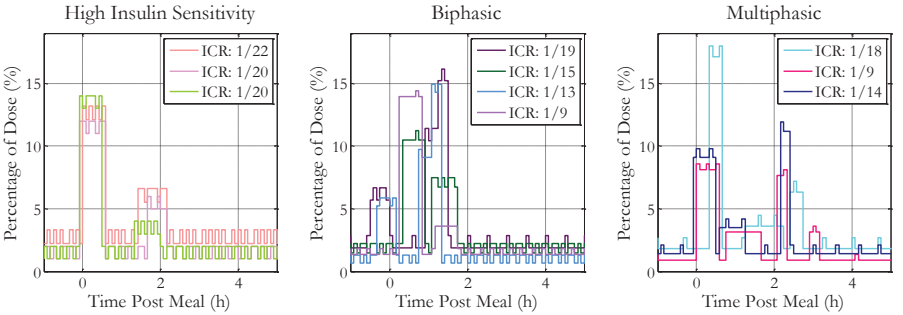

Figure 22. Observed trends in insulin profiles for ten *in silico* subjects. The left plot shows the group of *in silico* subjects with the highest insulin sensitivities and whose individual optimal insulin regimens are biphasic. The middle plot presents another group of subjects that have biphasic insulin delivery patterns, and the right plot shows the subjects whose insulin regimens are multiphasic.

The left hand side of Fig. 22 shows that the most consistent trend can be observed for the most insulin sensitive subjects with ICRs near 1/20. The regimens are very similar in terms of

the biphasic pattern and the time of insulin deliveries, which suggests that this may be an appropriate regimen for highly sensitive patients. However, no clear trend could be observed for subjects with lower insulin sensitivity. While most subjects are recommended a biphasic regimen, there are a few subjects that have multiphasic insulin profiles (right hand side of Fig. 22). Although it is natural that less sensitive subjects require multiple fast insulin deliveries to keep the blood glucose concentration from rising too high, no clear trend could be linked to the ICR. This is possibly because other factors, such as insulin absorption rate, also affect the appearance of the recommended regimens. However, for highly sensitive subjects the ICR seems to be the dominant factor.

To confirm the obtained results, the optimal regimens were compared to schemes that are currently offered by traditional insulin pumps.

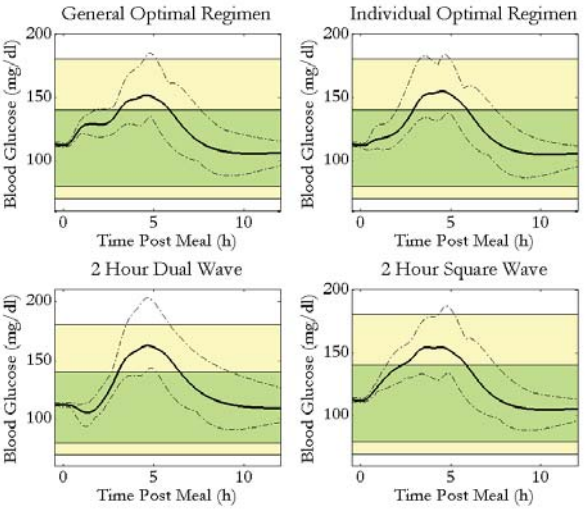

Figure 23. Comparison of insulin regimens for a pizza meal comprising 100 g of carbohydrates. The solid curves represent the average blood glucose profiles for ten i*n silico* subjects. The area between the dashed lines shows the range of variability.

Fig. 23 shows that it is difficult to distinguish the performance of the general, individual and square wave regimens since all three maintain most subjects within the range of 70 – 180 mg/dl with limited cases of hyperglycemia. The data presented in Table 3 provide a clearer comparison of the regimens.

Table 3. Comparison of various insulin regimens for a 100 g carbohydrate pizza meal

Insulin Regimen	Normalized AUC (mg/dl)	Mean % Time within 70-180 mg/dl	Mean % Time within 80-140 mg/dl	Mean Blood Glucose Peak (mg/dl)
General Regimen	8.5 ± 2.2	99.8 ± 0.7	91.7 ± 4.2	157.8 ± 15.6
Individual Regimen	8.0 ± 2.0	99.6 ± 0.8	91.3 ± 3.5	160.2 ± 15.3
Normal Bolus	12.7 ± 7.7	96.5 ± 6.5	84.2 ± 9.0	179.9 ± 23.3
2 Hour Dual Wave	9.1 ± 3.8	98.8 ± 2.6	88.9 ± 5.0	168.1 ± 18.7
2 Hour Square Wave	9.3 ± 2.1	99.6 ± 0.8	89.6 ± 4.5	161.3 ± 15.7

Table 3 shows that the individual optimal regimens perform better since they have a lower average AUC. The general and square wave regimens perform relatively well in terms of the percentage of time in euglycemia as well as the average blood glucose peak. However, the square wave regimen results in a significantly higher average AUC. Paired t-tests with an α-level of 0.05 were performed to compare the general and square wave regimens as well as the general and individual regimens, respectively. The statistical results reveal that the generalized optimal regimen performs significantly better than the square wave in terms of the time spent in euglycemia, the postprandial blood glucose peak as well as the normalized AUC. Furthermore, the statistical difference in performance between the general and individual regimens is insignificant, indicating that the general optimal regimen could be implemented as a common recommendation to patients when consuming similar meals.

The overall optimization results suggest biphasic regimens for larger high-fat pizza meals, while a square wave regimen appears to perform better for smaller meal sizes. The optimal regimens are all characterized by insulin deliveries within an approximate 2 hour postprandial period, independent of meal size.

Open-loop Regimens for High-fat Pasta Meals

Finally, the general optimal insulin regimens for high-fat pasta meals of various sizes were determined using PSO. The insulin regimens for meals comprising 50 and 75 g of carbohydrates can be found in Appendix B, and the general regimen for a 100 g carbohydrate high-fat pasta meal in Fig. 24.

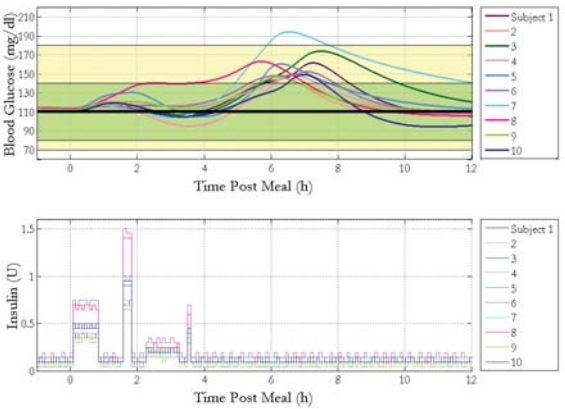

Figure 24. Generalized optimal open-loop insulin regimen for a high-fat pasta meal comprising 100 g of carbohydrates. The upper plot shows the postprandial blood glucose profiles for ten *in silico* subjects, and the bottom plot presents the optimal insulin deliver pattern for all ten subjects. The optimized delivery regimen maintains all but one subject in the 70-180 mg/dl safe zone despite the high carbohydrate content.

The result in Fig. 24 is an insulin regimen optimized for ten *in silico* subjects and comprises four consecutive waves of varying lengths. The recommended general regimen provides good blood glucose control for all ten *in silico* subjects, with all but one subject being maintained within the range of 70 – 180 mg/dl. However, it is important to recognize the difficulty of prescribing a general regimen for large meals since not all patients are equally sensitive to insulin. The general optimal regimens for 50 g and 75 g carbohydrate pasta meals are biphasic and triphasic, respectively. This indicates that the number of waves in the general regimen increases with meal size. The observed multiphasic insulin profiles are feasible considering the simulated glucose absorption profiles for high-fat pasta meals presented in Fig. 25.

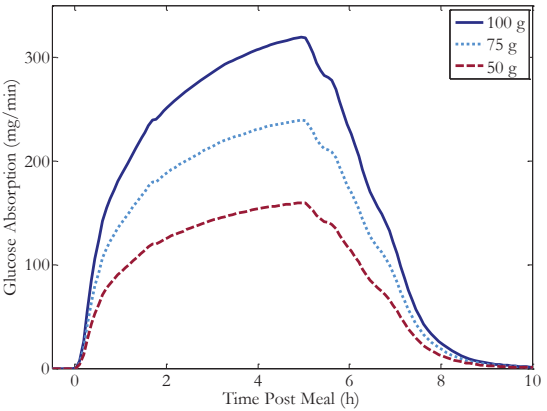

Figure 25. Ten subject average intestinal glucose absorption profiles for high-fat pasta meals comprising 50, 75, and 100 g of carbohydrates

The blood glucose peaks for the high-fat pasta meals occur approximately 6 hours after the start of the meal because the fat content in meals generally slow down glucose absorption. Since the rise in blood glucose is slow compared to the rate of insulin absorption and action, it seems appropriate to administer the insulin dose shortly after the start of the meal as suggested by the general optimal regimen in Fig. 24. Delivering insulin too early increases the risk for immediate hypoglycemia for this type of meal due to the slow glucose absorption. The optimization results propose regimens in which all the insulin deliveries are made within the first four hours after the start of the meal. This time interval is dependent on the time of the blood glucose peak that is similar for all meal sizes as shown in Fig. 25.The results also suggest that the number of waves in the regimen should increase with meal size, which can be explained by the relatively fast rise in blood glucose concentration resulting from larger meals. However, this is assuming that the meal duration is independent of meal size. The increasing number of waves is thus feasible since it is apparent that a faster increase in blood glucose requires multiple frequent deliveries of insulin to keep the blood glucose from rising too high. Smaller meals result in a slower rise in glucose which allows for longer gaps between the insulin deliveries.

Individual optimizations were also performed for the ten subjects with the aim of finding consistent trends that could be useful when prescribing insulin regimens to patients. The individual optimal insulin regimens for a 100 g high-fat pasta meal are presented in Fig. 26.

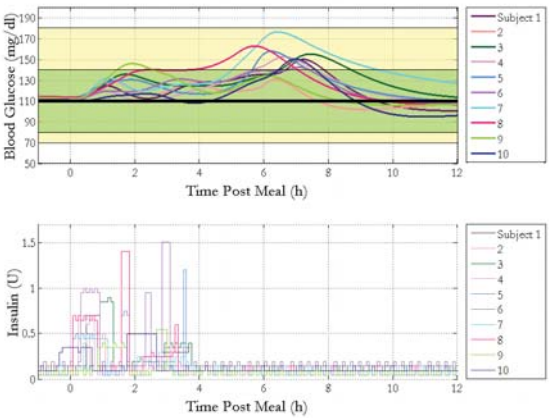

Figure 26. Individual optimal open-loop insulin regimens for a high-fat pasta meal comprising 100 g of carbohydrates. The upper plot shows the postprandial blood glucose profiles for ten *in silico* subjects, and the bottom plot presents the individual optimal insulin delivery patterns for all ten subjects.

These individual insulin regimens all have multiphasic patterns with the number of waves ranging from two to four. The patterns are similar to the general optimal regimen, with all insulin also being delivered within a four hour postprandial period. Fig. 27 presents the individual regimens together with the average insulin profile and offers a comparison between the average and general regimen.

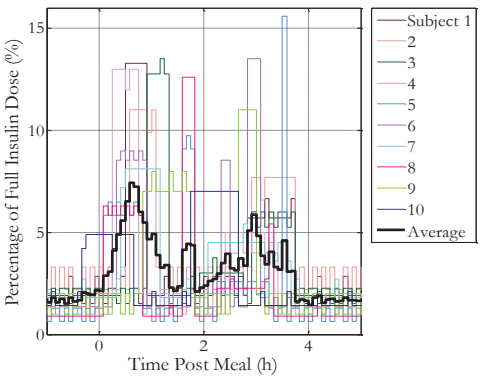

Figure 27a. The optimized individual delivery patterns for ten *in silico* subjects and the average insulin profile based on the ten individual patterns given a high-fat pasta meal comprising 100 g of carbohydrates.

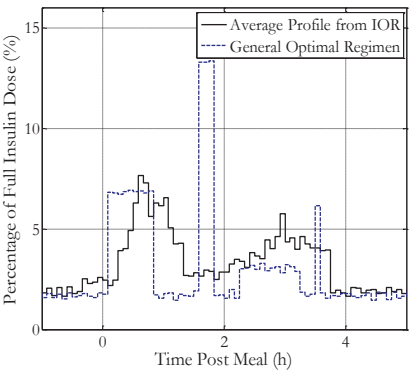

Figure 27b. Comparison between the average insulin profile based on individually optimized regimens (IOR) and the general regimen optimized for ten *in silico* subjects.

Fig. 27a shows the average insulin profile based on the individual optimal regimens, while a direct comparison of the average profile with the general optimal regimen is presented in Fig. 27b. This comparison clearly shows that the general regimen is reasonable since the insulin deliveries occur around the same time as the main peaks of the average insulin profile. The variations in insulin regimens are a result of many different factors which is why it is difficult to recognize clear trends in the proposed insulin regimens. However, one of the main factors in determining the regimen design appears to be the ICR. In Fig. 28, the individual optimal regimens for subjects with low ICR ($\leq 1/14$) and high ICR ($\geq 1/14$) are grouped to display the trends that occur due to differences in insulin sensitivity.

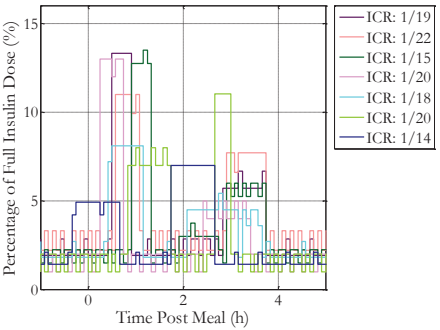

Figure 28a. Trends in individually optimized regimens for subjects with high insulin sensitivity. The plot shows a biphasic insulin delivery pattern for highly sensitive subjects.

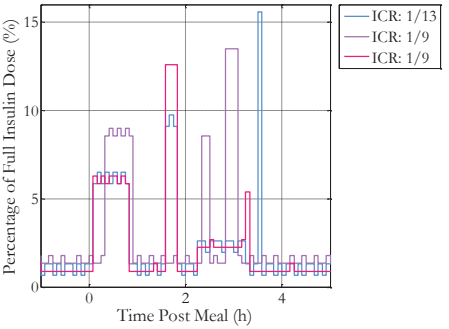

Figure 28b. Trends in individual optimal regimens for subjects with low insulin sensitivity. The plot shows multiphasic insulin delivery patterns for less sensitive subjects.

Although it is difficult to recognize clear trends in the insulin regimens, the most visible trend is that subjects with high insulin sensitivity (see Fig. 28a) are recommended a biphasic regimen. A clear trend for these subjects is that the first insulin wave is delivered within a two hour postprandial period, while the second wave is delivered between two and four hours after the start of the meal. However, one subject deviates from this time pattern, possibly due to the relatively low insulin sensitivity (ICR: 1/14). The biphasic regimens are realistic considering that multiple insulin waves might cause increased fluctuations in blood glucose concentration for sensitive subjects. Biphasic regimens with longer insulin waves provide slower insulin infusion, which is desirable for more sensitive patients. Fig. 28b shows that the individual optimal regimens for the less insulin sensitive subjects are multiphasic. The regimens are characterized by an initial long wave followed by short waves lasting up to 15 minutes. Intuitively, less sensitive subjects would require faster and more frequent insulin deliveries to keep the blood glucose from rising too high. This explains the higher number of short insulin spikes in the regimens presented in Fig. 28b.

To confirm that the obtained results are optimal, the general and individual regimens were compared to the ones currently offered by traditional insulin pumps. Fig. 29 compares the performance of the optimal insulin regimens for a 100 g pasta meal to that of a dual wave and square wave delivered at the time of the meal.

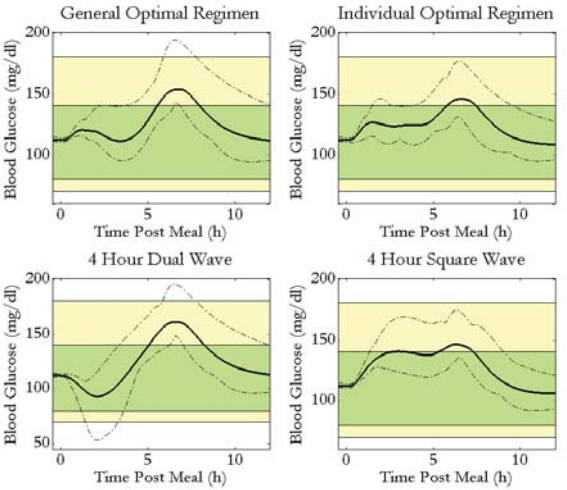

Figure 29. Comparison of insulin regimens for a high-fat pasta meal comprising 100 g of carbohydrates. The solid curves represent the average blood glucose profiles for ten *in silico* subjects. The area between the dashed lines shows the range of variability.

Fig. 29 shows that the general optimal regimen provides better control of the postprandial glucose excursion than a dual and square wave. The 4 hour dual wave results in hypo- and hyperglycemia for some subjects, while the 4 hour square wave performs relatively well. However, the upper blood glucose range for the square wave regimen is above 140 mg/dl for an extended period of time. The general optimal regimen is able to maintain euglycemia for a longer time period, although it is apparent that individualized optimal regimens result in better blood glucose control than the other suggested regimens for this meal type. Table 4 compares the performance of different regimens in terms of the normalized AUC, the percentage of time spent in the different blood glucose zones, as well as the glucose peak.

Table 4. Comparison of various insulin regimens for a 100 g carbohydrate pasta meal

Insulin Regimen	Normalized AUC (mg/dl)	Mean % Time within 70-180 mg/dl	Mean % Time within 80-140 mg/dl	Mean Blood Glucose Peak (mg/dl)
General Regimen	8.3 ± 4.0	99.4 ± 1.9	91.6 ± 6.2	159.3 ± 15.1
Individual Regimen	7.7 ± 2.7	100	94.3 ± 4.2	152.3 ± 12.1
Normal Bolus	18.9 ± 12.1	88.5 ± 9.1	75.5 ± 11.2	192.1 ± 33.6
4 Hour Dual Wave	9.8 ± 4.7	98.6 ± 3.9	88.5 ± 7.5	166.5 ± 14.1
4 Hour Square Wave	9.6 ± 2.9	100	90.4 ± 6.9	153.2 ± 12.5

The data presented in Table 4 show that the individualized optimal regimens result in overall better performance than the other regimens. This was also confirmed by a statistical t-test, which showed that the individual schemes perform significantly better than the general in terms of the time spent in euglycemia as well as the postprandial blood glucose peak. Although the 4 hour square wave performs relatively well, it is clear that the optimized regimens show consistently better performance since they yield average normalized AUCs below 9 mg/dl and the percentage of time in euglycemia is above 90%. However, the results from a statistical comparison between the general regimen and the square wave are inconclusive as they show no significant difference in performance, although the difference in normalized AUC is close to being significant. These results suggest the need for more extensive *in silico* testing with a larger subject population.

Even though the general regimen does not perform as well as the individual regimens, it is still able to maintain near-euglycemia for most *in silico* subjects with a relatively low average normalized AUC. With an overall good performance in comparison to the individual regimens, the general regimen could potentially be implemented as a common recommendation to patients when consuming similar meals.

The overall optimization results suggest that the best general insulin regimens for high-fat pasta meals of various sizes are multiphasic regimens. This was also confirmed by the individual optimization results. All the optimized regimens are characterized by insulin deliveries within a

four hour postprandial period with a varying number of insulin waves depending on the size of the meal.

Summary of Novel Open-loop Regimens

The particle swarm optimizations of open-loop insulin regimens yielded novel regimens for all three meal types studied. The optimal insulin delivery regimens for low-fat meals comprise a normal bolus or short square wave delivered at least 30 minutes prior to the meal, whereas the optimal regimens for pizza meals include square wave and biphasic regimens depending on the size of the meal. Furthermore, the optimal regimens for high-fat pasta meals are multiphasic where the number of waves increases with meal size. These optimized regimens demonstrated better performance in *in silico* trials than any pre-existing regimens currently offered by CSII therapy, and could therefore potentially be implemented as general recommendations for similar meals. Table 5 presents a summary of novel open-loop regimens for the 100 g meal scenarios, corresponding to the optimization results shown in Figs. 12, 18, and 24. The designs in Table 5 are expressed in terms of the starting time and duration of each square wave in the regimens as well as the percentage of the full insulin dose delivered. This percentage corresponds to the fraction of the full insulin dose, as calculated by the subject's ICR and the carbohydrate content in the meal. A library of the novel open-loop regimens for meals comprising 50 and 75 g of carbohydrates can be found in Appendix B.

Table 5. Novel open-loop regimens for meals comprising 100 g of carbohydrates

		Low-fat	**High-fat Pizza**	**High-fat Pasta**
Wave I	% of Insulin Dose	100	70	45
	Starting time (min)	-30	+20	+5
	Duration (min)	15	30	40
Wave II	% of Insulin Dose	-	30	35
	Starting time (min)	-	+60	+95
	Duration (min)	-	25	10
Wave III	% of Insulin Dose	-	-	15.5
	Starting time (min)	-	-	+135
	Duration (min)	-	-	55
Wave IV	% of Insulin Dose	-	-	4.5
	Starting time (min)	-	-	+210
	Duration (min)	-	-	0

4.2 Novel Closed-loop Insulin Regimens for Low and High-fat Meals

In the context of an artificial pancreas with meal announcements, it would be helpful to aid the controller with a fixed supplementary insulin regimen that is specific to a particular meal type and size. A PID controller was designed to study the two different closed-loop scenarios: simple PID control and PID control with a supplementary insulin regimen. The PSO method was used to determine the optimal controller parameters for the ten *in silico* subjects given a standard low-fat meal. Optimizations of the supplementary insulin regimens for three meal types of three different sizes were then performed with PID control.

Controller Parameter Optimization

The PSO algorithm was implemented to optimize the PID controller parameters, K_c, τ_I, and τ_D, for ten adult *in silico* subjects. The optimization was performed under the condition of a noisy subcutaneous sensor to obtain a more robust controller. The controller was tuned to a standard low-fat meal comprising 50 g of carbohydrates. The optimized parameters are presented in Table 6.

Table 6. Optimized controller parameters for a standard low-fat meal comprising 50 g of carbohydrates

Controller Parameter	Optimized Parameter Value
K_c [mg/dl]	-0.46
τ_I [s]	531.8
τ_D [s]	333.6

The performance of the designed PID controller using a noisy sensor is evaluated in Fig. 30.

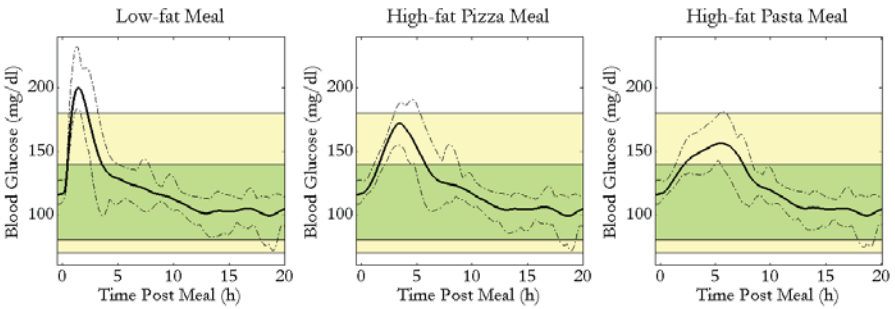

Figure 30. PID controller performance with noisy measurements for a low-fat, high-fat pizza, and high-fat pasta meal, each comprising 50 g of carbohydrates

The optimized PID controller performs well for high-fat meals with noisy measurements as shown in Fig. 30. However, it is not aggressive enough to avoid hyperglycemia for a low-fat meal due to the risk of hypoglycemia. The results suggest that controllers can provide better control of the postprandial glucose excursion following high-fat meals due to the slower rise and fall in glucose concentration, as long as the integral component is restricted. The given PID controller was used to evaluate the improvement in blood glucose control when combined with supplementary optimized insulin regimens for a variety of meals. This closed-loop strategy is illustrated in Fig. 31.

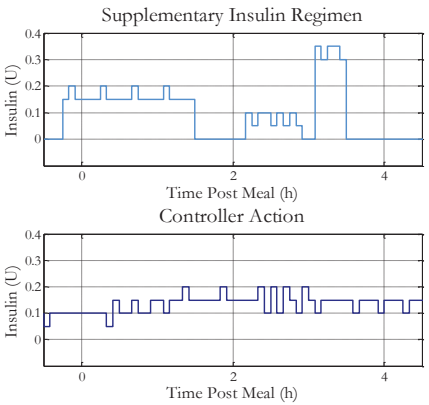

Figure 31. Illustration of closed-loop strategy with controller action combined with a supplementary optimized regimen, specific to a particular meal scenario.

The proposed closed-loop strategy is represented by a combination of PID control and a fixed insulin regimen that is optimized for a particular meal type and size, as shown in Fig. 31.

Closed-loop Regimens for Low-fat Meals

General closed-loop regimens comprising an optimized PID controller in combination with supplementary fixed regimens were optimized for ten *in silico* subjects using PSO. The meal scenarios studied were low-fat meals containing 50, 75, and 100 g of carbohydrates. The results for 50 and 75 g meals are presented in Appendix B, while the result for a 100 g low-fat meal is shown in Fig. 32.

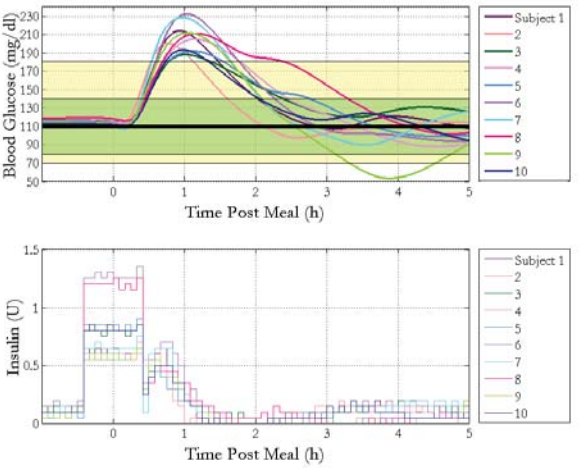

Figure 32. Generalized optimal closed-loop insulin regimen for a standard low-fat meal comprising 100 g of carbohydrates. The upper plot shows the postprandial blood glucose profiles for ten *in silico* subjects, and the bottom plot presents the insulin deliver pattern for all ten subjects.

The results presented in Fig. 32 suggest a supplementary regimen comprising a long square wave starting 30 minutes prior to the meal. However, this recommendation was obtained because the insulin delivery was constrained to 30 minutes before the meal. It is also important to note that the poor performance of the overall regimen is the result of a tuning issue and is not due to the meal type. This indicates that the controller tuning needs to be less aggressive for larger meals, and particularly fast absorbing meals, such as low-fat meals. The long square wave delivery is suggested as the optimal supplementary regimen to avoid postprandial hypoglycemia because the given controller is too aggressive for this particular meal. The results are clearly not optimal for this type of meal, and due to the poor performance, the results from this optimization were not analyzed further.

Closed-loop Regimens for High-fat Pizza Meals

Next, optimized general regimens for high-fat pizza meals of various sizes were found using PSO. The optimization result for a pizza meal comprising 100 g of carbohydrates is presented in Fig. 33, and the results for 50 and 75 g meals in Appendix B.

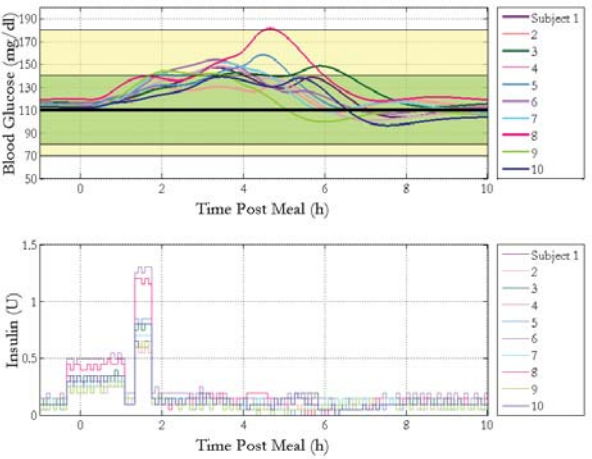

Figure 33. Generalized optimal closed-loop regimen for a high-fat pizza meal comprising 100 g of carbohydrates. The upper plot shows the postprandial blood glucose response profiles for ten *in silico* subjects, and the bottom plot presents the optimal insulin delivery pattern for all ten subjects. The delivery regimen maintains a majority of the subjects in euglycemia throughout the trial despite the high carbohydrate content.

The optimization results shown in Fig. 33 propose a closed-loop scheme comprising a supplementary biphasic regimen that maintains the blood glucose concentration within the 70-180 mg/dl safe zone for all subjects. The general regimens for 50 and 75 g pizza meals are similarly biphasic, but comprise a short square wave followed by a longer one. The biphasic patterns for all three meal sizes conform to the optimal open-loop schemes for this meal type in terms of the two hour postprandial insulin infusion, with minor regimen design variations. While the open-loop regimen for a 50 g meal comprises a long square wave, the closed-loop scheme is biphasic. This difference is possibly a result of limited initial control action due to the slow glucose excursion (see Fig. 19). The restricted control action imposes the need for fast insulin infusion, explaining the initial short wave in the closed-loop regimen for a 50 g pizza meal. The variations in regimen design for a 100 g pizza meal can be explained by the simulated glucose absorption profiles in Fig. 19 that show a faster rise in glucose concentration for larger meals. This rapid postprandial glucose excursion leads to higher initial derivative control action, which explains why the closed-loop insulin regimen for a 100 g pizza meal is initialized by slower

insulin infusion than the smaller meals.

To confirm the obtained results, the performance of the optimal closed-loop regimen was compared to that of simple PID control, the optimal open-loop regimen, and PID control with a supplementary 2 hour square wave regimen, as shown in Fig. 34.

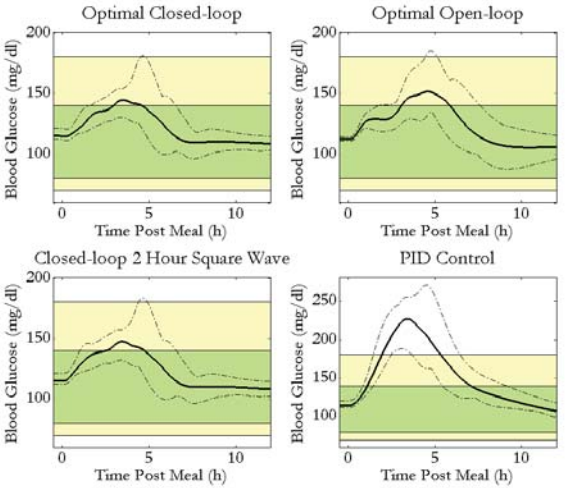

Figure 34. Comparison of insulin regimens for a high-fat pizza meal comprising 100 g of carbohydrates. The solid curves represent the average blood glucose profiles for ten *in silico* subjects. The area between the dashed lines shows the range of variability.

The results in Fig. 34 show that the closed-loop regimens provide significantly better control of the postprandial glucose excursion compared to simple PID control and the open-loop scheme. However, the performances of the two closed-loop regimens are nearly indistinguishable. Table 7 gives a clearer comparison of the different regimens in terms of the normalized AUC, average time in the safe zones, and the postprandial blood glucose peak.

Table 7. Comparison of various insulin regimens for a 100 g carbohydrate pizza meal

Insulin Regimen	Normalized AUC (mg/dl)	Mean % Time within 70-180 mg/dl	Mean % Time within 80-140 mg/dl	Mean Blood Glucose Peak (mg/dl)
Optimal Closed-loop	7.2 ± 1.7	100	95.0 ± 3.3	149.9 ± 13.1
Optimal Open-loop	8.5 ± 2.2	99.8 ± 0.7	91.7 ± 4.2	157.8 ± 15.6
Closed-loop 2 Hour Square Wave	7.9 ± 1.7	99.8 ± 0.5	92.5 ± 4.5	152.4 ± 13.3
PID Control	23.2 ± 5.9	89.6 ± 3.1	79.6 ± 6.4	229.7 ± 24.4

From the data presented in Table 7, it is apparent that the optimal closed-loop regimen performs better than other regimens since it results in a lower average normalized AUC, blood glucose peak and most importantly, no hyperglycemic events. This was also confirmed by statistical paired t-tests with an α-level of 0.05. Closed-loop control in combination with a supplementary square wave regimen seems to perform relatively well, but statistical tests show that the optimal closed-loop regimen is significantly better at controlling the postprandial blood glucose excursion indicated by the postprandial peak, time in euglycemia, and AUC. The promising results of the novel closed-loop strategy indicate that combining a controller with a supplementary optimized regimen can provide efficient control of postprandial blood glucose concentration following large meals.

The overall results suggest that the optimal closed-loop regimens for high-fat pizza meals are biphasic with the insulin dose delivered within a 2 hour postprandial period, independent of meal size.

Closed-loop Regimens for High-fat Pasta Meals

Finally, the PSO algorithm was also used to find the optimal closed-loop regimens for various high-fat pasta meals. The optimization results for meals comprising 50 and 75 g of carbohydrates are presented in Appendix B, and the result for a 100 g meal is shown in Fig. 35.

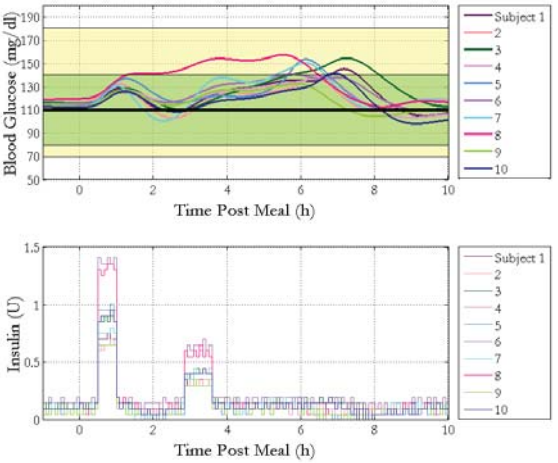

Figure 35. Generalized optimal closed-loop regimen for a high-fat pasta meal comprising 100 g of carbohydrates. The upper plot shows the postprandial blood glucose response profiles for ten *in silico* subjects, and the bottom plot presents the optimal insulin delivery pattern for all ten subjects. The delivery regimen maintains a majority of the subjects in euglycemia throughout the trial.

The optimal supplementary closed-loop regimen for a large high-fat pasta meal has a biphasic delivery pattern, as shown in Fig. 35. This closed-loop strategy maintains the blood glucose concentrations of all subjects within the safe zone of 70-180 mg/dl despite the high carbohydrate content. Interestingly, the optimal regimens for 50 and 75 g meals are triphasic, but are also extended over a 4 hour postprandial period. Meals comprising a larger amount of carbohydrates cause a faster rise in blood glucose, resulting in higher derivative action. This explains the extended biphasic pattern that is shown in Fig. 35, since increased control action reduces the need for frequent insulin waves. The closed-loop insulin delivery patterns for the smaller meal sizes are similar to the optimal open-loop regimens. However, the closed-loop design for the meal comprising 100 g of carbohydrates differs from the multiphasic open-loop regimen, and is possibly also a result of the significantly higher derivative action that can be observed for larger meals.

The performance of the optimized regimen was compared to that of simple PID control, the optimal open-loop regimen, and PID control with a supplementary 4 hour square wave, as shown in Fig. 36.

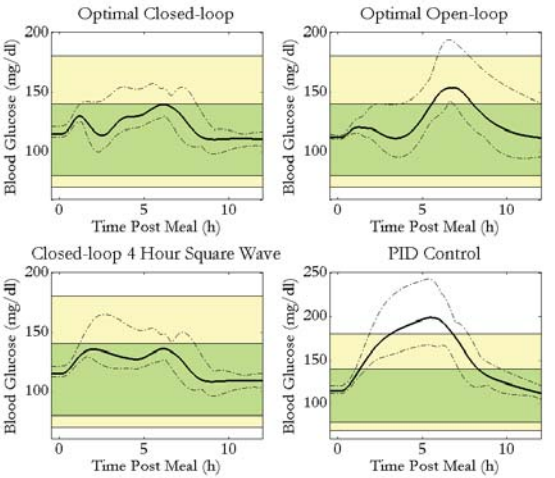

Figure 36. Comparison of insulin regimens for a high-fat pasta meal comprising 100 g of carbohydrates. The solid curves represent the average blood glucose profiles for ten *in silico* subjects. The area between the dashed lines shows the range of variability.

The results in Fig. 36 suggest that the optimal closed-loop regimen performs better than other regimens since it maintains near-euglycemia for all subjects. Although the closed-loop scheme with a 4 hour square wave performs comparatively well, the upper glucose range for the regimen is well above 140 mg/dl for an extended time period and appears to result in larger deviations from the baseline of 110 mg/dl. Table 8 compares these regimens based on the average normalized AUC, the postprandial peak, and other performance metrics.

Table 8. Comparison of various insulin regimens for a 100 g carbohydrate pasta meal

Insulin Regimen	Normalized AUC (mg/dl)	Mean % Time within 70-180 mg/dl	Mean % Time within 80-140 mg/dl	Mean Blood Glucose Peak (mg/dl)
Optimal Closed-loop	6.8 ± 1.7	100	96.3 ± 5.3	144.8 ± 8.3
Optimal Open-loop	8.3 ± 4.0	99.4 ± 1.9	91.6 ± 6.2	159.3 ± 15.1
Closed-loop 4 Hour Square Wave	7.4 ± 1.5	100	96.7 ± 5.2	143.0 ± 9.4
PID Control	23.0 ± 5.9	89.9 ± 5.8	76.2 ± 5.4	199.7 ± 22.9

The results shown in Table 8 indicate that closed-loop regimens with supplementary optimized regimens are more efficient in controlling postprandial blood glucose concentration than open-loop regimens, which was also confirmed by a statistical paired-test. The two closed-loop strategies with supplementary regimens perform similarly well, as they result in similar average blood glucose peaks and percentage of time in the safe zones. However, the optimized regimen produces a significantly lower AUC, implying overall less deviation from the baseline. Statistical tests confirm that the optimal closed-loop regimen performs significantly better than the closed-loop regimen involving a 4 hour square wave in terms of the AUC. The data thus suggests that a closed-loop strategy with an optimized supplementary regimen is an effective method of controlling the postprandial blood glucose excursion following a large meal.

The optimization results propose triphasic closed-loop regimens for small to medium sized high-fat pasta meals, and biphasic delivery patterns for large meals. All the novel regimens for this type of meal are characterized by insulin deliveries over a 4 hour postprandial period.

Summary of Novel Closed-loop Regimens

The optimizations of closed-loop insulin delivery regimens for various meal types produced novel supplementary regimens that can assist controllers in providing efficient control of postprandial blood glucose excursions following large meals. The optimal insulin delivery regimens for low-fat meals comprise a normal bolus or a short square wave depending on the size of the meal. Due to a controller tuning issue, the optimal regimen for large low-fat meals could not be determined. While the optimal closed-loop schemes for pizza meals seem to follow a biphasic pattern, the regimens for high-fat pasta meals are either bi- or triphasic depending on the meal size. The performances of these optimized schemes were superior to closed-loop control combined with supplementary existing regimens, such as square waves. This suggests that closed-loop PID control in combination with an optimized supplementary insulin delivery regimen is an efficient compensation strategy for large meals. As this type of scheme does not rely on optimized basal rates, it is a realistic approach that could potentially have real-life applications in an artificial pancreas. Table 9 shows a summary of novel closed-loop regimens for the 100 g meal scenarios, while a library of schemes for 50 and 75 g meals can be found in Appendix B.

Table 9. Novel supplementary regimens in a closed-loop setting for meals comprising 100 g of carbohydrates

		High-fat Pizza	**High-fat Pasta**
Wave I	% of Insulin Dose	51	64
	Starting time (min)	-20	+30
	Duration (min)	80	25
Wave II	% of Insulin Dose	48	36
	Starting time (min)	+80	+170
	Duration (min)	20	40
Wave III	% of Insulin Dose	-	-
	Starting time (min)	-	-
	Duration (min)	-	-
Wave IV	% of Insulin Dose	-	-
	Starting time (min)	-	-
	Duration (min)	-	-

5. Robustness Analysis

Both closed-loop and conventional CSII with user announcements require a number of parameter estimates, including meal size and ICR. This gives rise to uncertainties in the insulin dose and could potentially cause postprandial hyper- or hypoglycemia due to over- or under-delivery of insulin. Therefore, it is important that the insulin delivery regimen is robust to uncertainties in various factors. The robustness of each novel regimen was evaluated in terms of its sensitivity to errors in meal and ICR estimates.

5.1 Regimens for Low-fat Meals

A robustness analysis was performed for three different regimens for a low-fat meal comprising 100 g of carbohydrates. In Table 6, two novel regimens are compared to a normal bolus delivered 30 minutes prior to the meal as this pre-existing regimen showed similar performance to the novel open-loop regimen (see Chap. 4.1 Novel Open-loop Insulin Regimens for Low- and High-fat Meals).

Table 6. Robustness analysis results for a normal bolus and two novel insulin regimens given a low-fat meal comprising 100 g of carbohydrates.

Regimens		**Meal Size Estimate**			**I:C Ratio estimate**		
		-25%	Nominal	+25%	-25%	Nominal	+25%
Normal Bolus 30 minutes Prior to Meal	% Time in Hyperglycemia	8.2±3.9	2.4±2.7	0	6.4±4.5	2.4±2.7	0.2±0.6
	% Time in Hypoglycemia	0.03±0.1	0.03±0.1	0.05±0.2	0	0.03±0.1	0.08±0.3
	Blood Glucose Peak (mg/dl)	224±24.3	185±14.7	155±10.3	208±21.9	185±14.7	168±12.8
	Normalized AUC (mg/dl)	15.4±6.3	9.8±2.2	7.8±2.3	13.9±6.3	9.8±2.2	9.8±3.0
Optimal Open-loop	% Time in Hyperglycemia	7.2±3.1	2.4±2.5	0	5.9±4.0	2.4±2.5	0.2±0.6
	% Time in Hypoglycemia	0	0	0	0	0	2.2±3.8
	Blood Glucose Peak (mg/dl)	225±21.9	187±13.9	158±10.3	208±20.2	187±13.9	172±12.7
	Normalized AUC (mg/dl)	14.3±4.5	9.9±2.1	8.8±2.7	13.0±5.0	9.9±2.1	11.2±3.6
Optimal Closed-loop	% Time in Hyperglycemia	4.8±1.3	2.8±1.3	0.4±0.7	4.0±1.4	2.8±1.3	1.6±1.1
	% Time in Hypoglycemia	0.4±1.3	0.3±1.0	0.2±0.7	0	0.3±1.0	0.5±1.6
	Blood Glucose Peak (mg/dl)	236±19.3	202±14.0	175±10.8	216±16.5	202±14.0	191±13.1
	Normalized AUC (mg/dl)	11.7±2.3	8.0±1.2	6.6±1.3	10.1±1.9	8.0±1.2	7.8±1.6

The results in Table 6 show that the novel open-loop regimen has comparable robustness to the existing regimen. Interestingly, the novel regimen appears to be more robust to errors in the meal size estimate than the normal bolus delivered 30 minutes prior to the meal as it results in less hyper- and hypoglycemic events. Statistical paired t-tests with an α-level of 0.05 also show that the novel open-loop regimen is generally significantly more robust than the normal bolus. Overall, for large fast absorbing meals, the closed-loop performs worse than the open-loop regimens due to a controller tuning issue. However, the low standard deviation and small variations in performance across the different scenarios suggest that a correctly tuned controller in combination with an optimized supplementary regimen will be more robust to uncertainties in the meal size and ICR compared to open-loop therapy.

5.2 Regimens for High-fat Pizza Meals

Next, three insulin regimens for a high-fat pizza meal were evaluated in terms of their robustness to errors in meal size and ICR estimates. The results from the analysis are presented in Table 7, which compares the performance of two novel regimens and a 2 hour square wave.

Table 7. Robustness analysis results for a 2 hour square wave and two novel insulin regimens given a high-fat pizza meal comprising 100 g of carbohydrates.

Regimens		**Meal Size Estimate**			**I:C Ratio estimate**		
		-25%	Nominal	+25%	-25%	Nominal	+25%
2 Hour Square Wave	% Time in Hyperglycemia	6.4±5.2	0.4±0.8	0	4.1±4.9	0.4±0.8	0
	% Time in Hypoglycemia	0	0	0	0	0	0
	Blood Glucose Peak (mg/dl)	197±26.3	161±15.7	135±8.9	188±24.3	161±15.7	142±11.1
	Normalized AUC (mg/dl)	15.5±6.3	9.3±2.1	6.4±1.8	14.2±6.4	9.3±2.1	8.0±2.2
Optimal Open-loop	% Time in Hyperglycemia	4.8±4.7	0.2±0.7	0	2.9±4.6	0.2±0.7	0
	% Time in Hypoglycemia	0	0	0	0	0	0
	Blood Glucose Peak (mg/dl)	193±25.8	158±15.6	131±8.1	183±23.3	158±15.6	138±11.0
	Normalized AUC (mg/dl)	14.7±6.3	8.5±2.2	5.6±1.7	13.4±6.2	8.5±2.2	7.0±2.2
Optimal Closed-loop	% Time in Hyperglycemia	0.8±2.0	0.08±0.3	0	0.4±1.4	0.08±0.3	0
	% Time in Hypoglycemia	0	0	0	0	0	0
	Blood Glucose Peak (mg/dl)	173±17.7	150±13.2	132±9.2	165±15.5	150±13.2	138±10.9
	Normalized AUC (mg/dl)	11.3±2.5	7.2±1.7	4.8±1.6	10.0±2.4	7.2±1.7	5.5±1.4

Table 7 shows that the optimal open-loop regimen is more robust to uncertainties in meal size and ICR compared to a 2 hour square wave. A statistical paired t-test with an α-level of 0.05 also confirmed that the novel open-loop regimen is significantly more robust. The novel regimen results in fewer hyperglycemic events and maintains comparatively lower blood glucose peaks and normalized AUC for the different scenarios. The overall better performance of the general optimal regimen suggests that it could provide better control of postprandial glucose concentration for large pizza meals compared to pre-existing delivery patterns. The optimized

closed-loop scheme performs better than the two open-loop regimens for the nominal case since it results in considerably lower AUC, blood glucose peaks, and fewer hyperglycemic events. Statistical tests also show that the novel closed-loop regimen is significantly more robust to errors in meal size and ICR estimates compared to the open-loop schemes. The closed-loop strategy also displays significantly lower standard deviations for all measured parameters, indicating that the regimen is robust to inter-subject variability.

5.3 Regimens for High-fat Pasta Meals

Finally, the robustness of a 4 hour square wave and two novel regimens was evaluated in terms of their sensitivity to perturbations in meal size and ICR estimates for high-fat pasta meals. Table 8 compares the performance of these three regimens for various scenarios.

Table 8. Robustness analysis results for a 4 hour square wave and two novel insulin regimens given a high-fat pasta meal comprising 100 g of carbohydrates.

Regimens		**Meal Size Estimate**			**I:C Ratio estimate**		
		-25%	Nominal	+25%	-25%	Nominal	+25%
4 Hour Square Wave	% Time in Hyperglycemia	4.4±7.0	0	0	3.5±6.1	0	0
	% Time in Hypoglycemia	0	0	0	0	0	0
	Blood Glucose Peak (mg/dl)	185±22.3	153±12.5	132±7.8	177±21.2	153±12.5	138±9.4
	Normalized AUC (mg/dl)	16.2±7.0	9.6±2.9	6.2±2.4	14.8±6.9	9.6±2.9	7.6±3.0
Optimal Open-loop Regimen	% Time in Hyperglycemia	4.3±6.5	0.6±1.9	0	3.0±5.5	0.6±1.9	0
	% Time in Hypoglycemia	0	0	0	0	0	1.6±2.7
	Blood Glucose Peak (mg/dl)	192±24.9	159±15.1	127±9.3	181±21.8	159±15.1	136±10.5
	Normalized AUC (mg/dl)	15.5±8.7	8.2±4.1	6.7±3.2	14.0±7.6	8.2±4.1	7.5±3.1
Optimal Closed-loop Regimen	% Time in Hyperglycemia	0.1±0.4	0	0	0	0	0
	% Time in Hypoglycemia	0	0	0	0	0	0
	Blood Glucose Peak (mg/dl)	163±11.7	145±8.3	130±5.4	156±10.5	145±8.3	134±6.4
	Normalized AUC (mg/dl)	10.9±2.5	6.8±1.7	4.8±1.6	9.8±2.4	6.8±1.7	5.3±1.6

The results from the analysis show that the novel open-loop scheme is similarly robust to errors in meal size and ICR estimates as the 4 hour square wave and was also confirmed by statistical tests. The performances of both regimens across the various scenarios are comparable in terms of the average time in hyperglycemia, but the novel regimen results in overall lower AUCs. The novel closed-loop regimen provides significantly better postprandial glucose control since it maintains lower blood glucose peaks and results in a negligible number of hyperglycemic events. The AUC and standard deviations are also considerably low for this regimen, indicating that it is a generally more robust method. Statistical tests also show that the closed-loop regimen is a comparatively more robust to errors in meal size and ICR estimates.

The overall results from the robustness analysis of insulin regimens for all three meal types show that the novel open-loop schemes are more or similarly robust to uncertainties in meal size

and ICR estimates as existing schemes. The data also indicates that closed-loop regimens comprising a PID controller in combination with a supplementary optimized regimen are more robust since the variation in performance over the different scenarios is relatively small. This type of scheme does not rely on optimal basal therapy and is thus a more realistic strategy that could potentially have real-life applications in an artificial pancreas.

6. Discussion

The insulin delivery profile for a standard meal in conventional basal-bolus therapy comprises a normal bolus (Jones et al., 2005). The performances of the novel open- and closed-loop insulin regimens were therefore compared to this bolus type (see Appendix B). The comparison made in Fig. B3 shows that the novel regimens perform significantly better than the normal bolus for all 9 meal scenarios with lower postprandial peaks, longer time spent in euglycemia, and less deviations from the baseline concentration of 110 mg/dl. In simulation trials, the normal bolus demonstrates adequate performance for fast absorbing low-fat meals, but does not appear to be the optimal compensation method for slow absorbing high-fat meals. This confirms recently published clinical data by Chase et al. (2002) and Jones et al. (2005). These studies suggest that insulin delivered as a dual wave is the optimal scheme for high-fat meals. However, this finding is based on performance comparisons of a limited number of schemes. The other types of insulin regimens that have been considered for such meals are the traditional normal bolus and square wave bolus, but they have not been as successful at attenuating the postprandial blood glucose peak as the dual wave (Chase et al., 2002). Since other types of delivery profiles have not yet been explored, it has not been possible to verify that the dual wave is in fact the optimal regimen for high-fat meals.

The results obtained in this simulation study indicate that regimens with slower insulin infusion rates provide better attenuation of the postprandial glucose excursions following high-fat meals. This confirms previous findings by Jones et. al (2005) and Chase et al.(2002). However, the novel regimen designs differ from traditional bolusing schemes as they comprise unique waveforms that are either bi- or multiphasic. Although the dual wave bolus is currently considered the optimal regimen for high-fat meals, the novel open- and closed-loop regimens generated in this study show superior postprandial control in *in silico* trials. Furthermore, these trials proved them to be more or similarly robust to uncertainties in meal size and ICR estimates as existing schemes.

Although the novel regimens show promising results in controlling postprandial blood glucose concentrations, the optimization problem framework could be improved to allow other types of delivery patterns that are not restricted to a multiple wave pattern. However, this would result in a large number of variables and extremely long computation time. Consequently, an alternative optimization approach would be necessary to produce more flexible insulin delivery designs. The insulin regimen library constructed in this study could also be extended with access to more clinical data on the postprandial glucose responses to high-fat meals in people with type

1 diabetes. Through *in silico* replication of additional data, it would be possible to find optimal insulin delivery patterns for a larger variety of meal compositions. Additionally, although the *in silico* trials were successful, an even more interesting evaluation of the novel insulin regimens would be that of a clinical trial. This would be necessary to confirm the *in silico* results and is required before considering practical applications of the novel regimens proposed in this study.

For long term goals, other hormones that influence meal absorption can also be utilized to improve overall meal compensation. Pramlintide is an analogue of the hormone amylin that decreases the meal absorption rate, and an optimized insulin and pramlintide delivery model that takes into account administration of both hormones may be the key in further improving postprandial blood glucose control. Ultimately, the optimization approach developed for the duration of this project is robust and widely applicable to other areas of the artificial pancreas, and has laid the groundwork for efforts that incorporate similar approaches in controller and model parameter estimations.

7. Conclusions

A model of the glucose-insulin dynamics in a person with type 1 diabetes mellitus currently implemented in the FDA-accepted UVA/Padova metabolic simulator was modified to allow simulation of meals of different absorption rates. This modification was utilized for extensive evaluation of multiple novel insulin regimens under meals with varied fat content. Simulations of high-fat meals under this modified model demonstrated qualitative replications of published data. Subsequently, an insulin regimen library with novel meal compensation strategies for a variety of meal compositions was constructed using the particle swarm optimization methodology.

Solving these optimization problems yielded novel open- and closed-loop regimens that provide better control of the postprandial glucose excursions than existing schemes. These novel delivery patterns comprise unique waveforms that are not available in existing insulin pump wizards as they have very limited bolus options, mainly normal bolus, dual wave, and square wave. The optimization results show that the theoretically optimal open-loop insulin delivery regimens for low-fat meals comprise a normal bolus or a short square wave delivered at least 30 minutes prior to the meal. However, it is important to consider the risks associated with early insulin deliveries. Optimal regimens for high-fat meals are typically biphasic, but can extend to multiple phases depending on the meal absorption rate and carbohydrate content. Individually tailored optimizations demonstrate a clear trend for subjects with high insulin sensitivity, suggesting that these patients should follow a biphasic insulin delivery for high-fat meals. Preliminary investigations of the optimal closed-loop regimens under varied fat content also display bi- or triphasic patterns for high-fat meals and are primarily influenced by the carbohydrate content in the meal.

The robustness analysis of the novel strategies revealed that the open-loop regimens are more or similarly robust to uncertainties in meal size and ICR estimates as existing schemes. However, novel closed-loop designs with supplementary optimized regimens are significantly more robust as determined by minimal inter-subject variability as well as improved overall control performance. Since this scheme does not rely on individually optimized basal rates, it is a more realistic strategy that could have real-life applications in an artificial pancreas.

8. References

Aronoff, S. L., Berkowitz, K., Shreiner, B., Want, L. (2004). Glucose Metabolism and Regulation: Beyond Insulin and Glucagon. *Diabetes Spectrum*, *17*(3), 183-190.

Chase, H. P., Saib, S. Z., MacKenzie, T., Hansen, M. M. Garg, S. K. (2002). Post-prandial Glucose Excursions Following Four Methods of Bolus Insulin Administration in Subjects with Type 1 Diabetes. *Diabetic Medicine*, *19*(4), 317-321.

Cobelli, C., Renard, E., Kovatchev, B. (2011). Artificial Pancreas: Past, Present, Future. *Diabetes*, *60*, 2672-2682.

Dalla Man, C., Cobelli, C. (2006). A System Model of Oral Glucose Absorption: Validation on Gold Standard Data. *IEEE Transactions on Biomedical Engineering*, *53*(12), 2472-2478.

Dalla Man, C., Rizza, R.A., Cobelli, C. (2007). Meal Simulation Model of the Glucose-Insulin System. *IEEE Transactions on Biomedical Engineering*, *54*(10), 1740-1749.

Daneman, D. (2006). Type 1 Diabetes. *The Lancet Diabetes & Endocrinology*, *367*, 847-58.

Dassau, E., Zisser, H., Harvey, R. A., Percival, M. W., Grosman, B., Bevier, W., . . . Doyle III, F. J. (2013). Clinical Evaluation of a Personalized Artificial Pancreas. *Diabetes Care*, *36*(4), 901-809.

Doyle, F., Jovanovic, L., Seborg, D., Parker, R. S., Bequette, B. W., Jeffrey, A. M., . . . McAvoy, T. (2007). A Tutorial on Biomedical Process Control. *Journal of Process Control*, *17*, 571-594

Farmer, T., Edgar, T., Peppas, N. (2008). The Future of Open- and Closed-loop Insulin Delivery Systems. *Journal of Pharmacy and Pharmacology*, *60*(1), 1-13.

Galgani, J., Aguirre, C., Díaz, E. (2006). Acute Effect of Meal Glycemic Index and Glycemic Load on Blood Glucose and Insulin Responses in Humans. *Nutrition Journal*, *5*, 22-28.

Herrero, P., Palerm, C. C., Dassau, E., Zisser, H., Jovanovic, L., Dalla Man, C., Cobelli, C., Vehi, J., Doyle III , F. J. "A Glucose Absorption Model Library of Mixed Meals for In-Silico Evaluation of Artificial β-Cell Control Algorithms". Presentation at the Annual Diabetes Technology Meeting, San Francisco, CA, October 25-27, 2007.

International Diabetes Federation (2012). *The Global Burden*.
Retrieved from http://www.idf.org/diabetesatlas/5e/the-global-burden

International Diabetes Federation (2013). *IDF Diabetes Atlas Update 2012*.
Retrieved from http://www.idf.org/diabetesatlas/5e/Update2012

Kennedy, J., Eberhart, R. (1995). 'Particle Swarm Optimization', in proceedings of IEEE International Conference on Neural Networks, *4*, 1942-1948.

Kumareswaran, K., Evans, M. L., Hovorka, R. (2012). Closed-loop Insulin Delivery: Towards Improved Diabetes Care. *Discovery Medicine*, *69*.

Liu, S., Huang, H., Lin, C., Chien, I. (2013). Fuzzy-Logic-Based Supervisor of Insulin Bolus Delivery for Patients with Type 1 Diabetes Mellitus. *Industrial and Engineering Chemistry Research*, *52*, 1678-1690.

Marieb, E. N., Hoehn, K. N. (2000). *Human Anatomy and Physiology*. San Francisco, USA: Benjamin-Cummings Publishing Company.

McMillin, J.M. (1990). Clinical Methods: The History, Physical, and Laboratory Examinations, 3rd edition. In Walker, H. K., Hall, W. D., and Hurst, J. W. (Eds.), *Chapter 141: Blood Glucose*. Boston: Butterworths.

Normand, S., Khalfallah, Y., Louche-Pelissier, C., Antoine, J. M., Blanc, S., Desage, M., Riou, J. P., Laville, M. (2001). Influence of Dietary Fat on Postprandial Glucose Metabolism Using Intrinsically ^{13}C-Enriched Durum Wheat. British Journal of Nutrition, *86*(1), 3-11.

Pankowska, E., Blazik, M., Groele, L. (2012). Does the Fat-Protein Meal Increase Postprandial Glucose Level in Type 1 Diabetes Patients on Insulin Pump: the Conclusion of a Randomized Study. *Diabetes Technology and Therapeutics*, *14*(1), 16-22.

Rubin, A. L. (2008). *Type 1 Diabetes for Dummies*. Hoboken, NJ: Wiley Publishing, Inc.

Scaramuzza, A. E., Iafusco, D., Giani, E., Spiri, D., De Palma, A., Bosetti, A., . . . Zuccotti, G. V. (2007). 'The Optimal Type of Bolus Following a Pizza Meal in Children and Adolescents with Type 1 Diabetes', in the 43rd General Assembly of the European Association for the Study of Diabetes, Amsterdam, Netherlands.

Shrayyef, M., Gerich, J. (2010). Principles of Diabetes Mellitus. In Poretsky, L. (Ed.), *Normal Glucose Homeostasis* (pp. 19-35). New York, NY: Springer.

Soru, P., Nicolao, G. D., Toffanin, C., Dalla Man, C., Cobelli, C., Magni, L. (2012). MPC Based Artificial Pancreas: Strategies for Individualization and Meal Compensation. *Annual Reviews in Control*, *36*(1), 118-128.

Stemmann, M. (2013). *Predictive Control of Diabetic Glycemia*. Licentiate thesis, Lund University.

Univ. of Maryland, Medical Center (2013). *Diabetes - Type 1*. Retrieved from http://umm.edu/health/medical/reports/articles/diabetes-type-1

Williamson, P. (2011). *Exercise for Special Populations*. MD, USA: Lippincott Williams & Wilkins.

World Health Organization (2013). *Diabetes*. Retrieved from http://www.who.int/en/

Zisser, H., Wagner, R., Pleus, S., Haug, C., Jendrike, N., Parkin, C., Schweitzer, M., Freckmann, G. (2010). Clinical Performance of Three Bolus Calculators in Subjects with Type 1 Diabetes Mellitus: A Head-to-Head-to-Head Comparison. *Diabetes Technology and Therapeutics*, *12*(12), 955-961.

Appendix A

Computational Parameters in the Insulin Regimen Optimization

This chapter serves to further explain the insulin regimen optimization and design for each meal scenario.

The insulin regimen was designed as a multiple delivery scheme with four possible doses. The optimization variables are the time of each insulin delivery, the duration of each delivery, and the fraction of the full insulin dose to be administered with each delivery. The lower and upper limits for each variable are given in Table A1.

Table A1. Lower and upper limits for the optimization variables

	Lower Limit	Upper Limit
Time of Delivery (min)	- 30	+ 300
Duration of Delivery (min)	0	+ 150
Fraction of Full Dose	0	1

In addition to the specified limits, the insulin dosage was restricted to the calculated full insulin dose as determined by Eq. 1. The dosage constraint is presented in Eq. A1.

$$\sum_{i}^{n=4} x_i \leq 1 \tag{A1}$$

, where i denotes a specific dose in the optimized multiple delivery regimen and x_i is the fraction of the full insulin dose administered with the i^{th} delivery.

The various insulin regimens were optimized based on the cost function in Eq. A2.

$$f = \frac{100}{\%\ \text{of time in}\ 80\ -140\ \text{mg/dl}} + \frac{\%\ \text{of time below 70 mg/dl}}{100} + \sum_{i}^{n} (BG_i - 110)^2 \qquad (A2)$$

, where the percentage of time in hypo- and euglycemia was calculated as an average for ten *in silico* subjects. The last term in Eq. A2 represents the residual sum of squares where i denotes a specific data point in a system with a discrete time step of five minutes, and the variable BG_i is the i^{th} recorded average blood glucose concentration in simulation. The cost function was designed to maximize the time spent in euglycemia, minimize the time in hypoglycemia, and reduce the deviation from the baseline of 110 mg/dl.

Appendix B

Novel Insulin Regimens

This chapter presents the novel open- and closed-loop insulin regimens that were obtained through optimization using the Particle Swarm Optimization algorithm.

The novel regimens for three different meal types are presented in Figs. B1 and B2. Fig. B1 shows the open-loop regimens for 9 meal scenarios, and the closed-loop regimens for the same scenarios are shown in Fig. B2. Fig. B3 demonstrates a performance comparison between the novel regimens and the conventional insulin delivery profile for a standard meal.

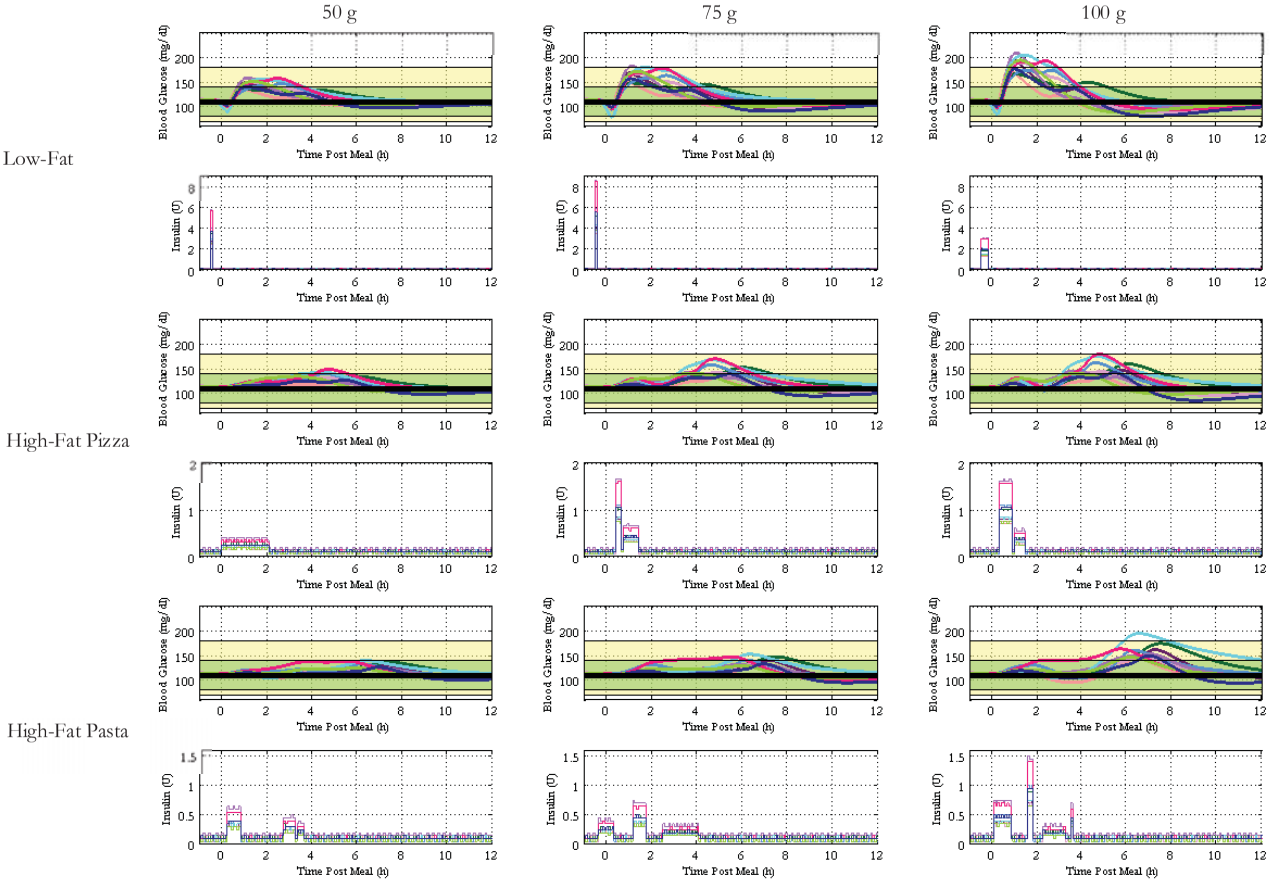

Figure B1. Summary of optimized general open-loop regimens for three different meal types of various sizes. The figure shows the blood glucose response profiles and insulin delivery patterns for ten *in silico* subjects given 9 different meal scenarios.

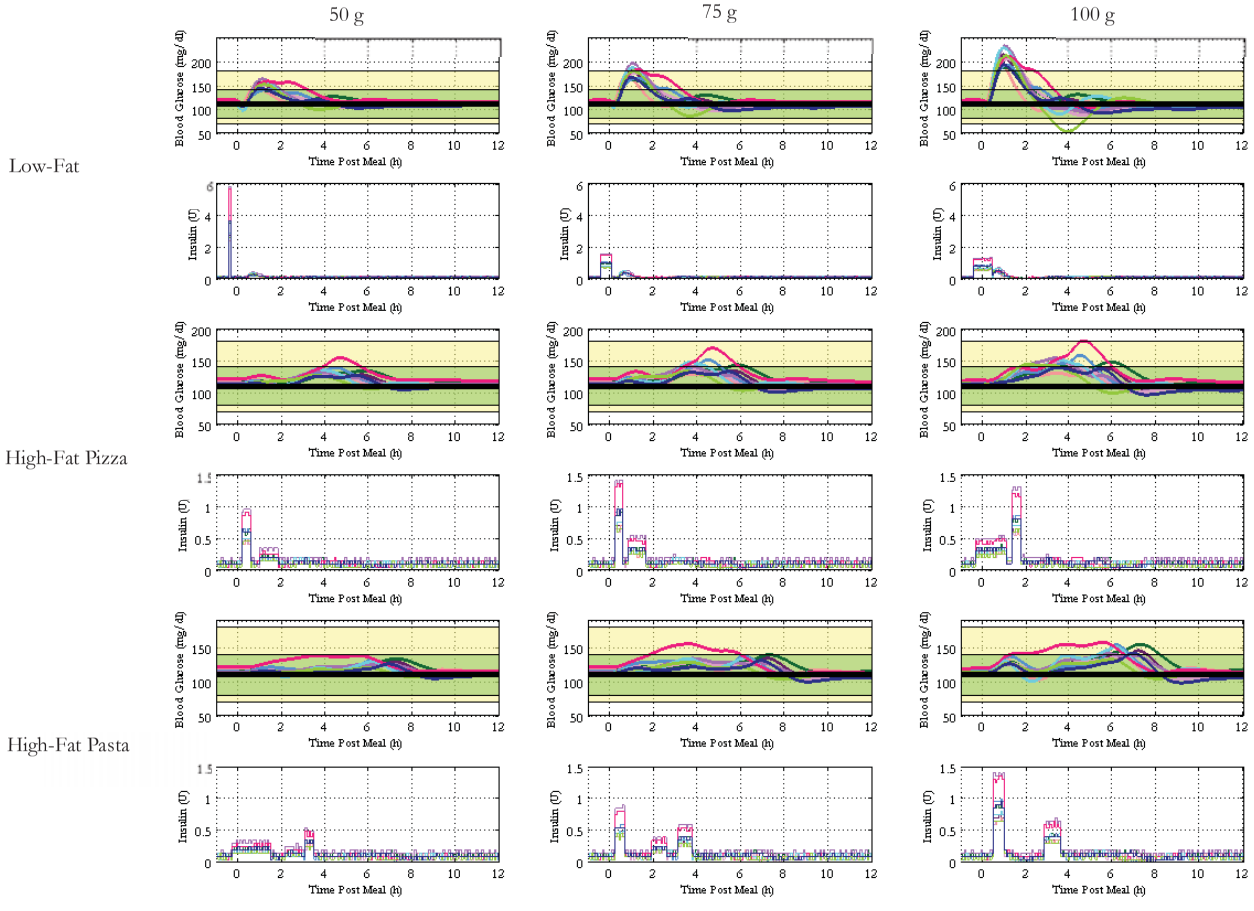

Figure B2. Summary of optimized general closed-loop regimens for three different meal types of various sizes. The figure shows the blood glucose response profiles and insulin delivery patterns for ten *in silico* subjects given 9 different meal scenarios.

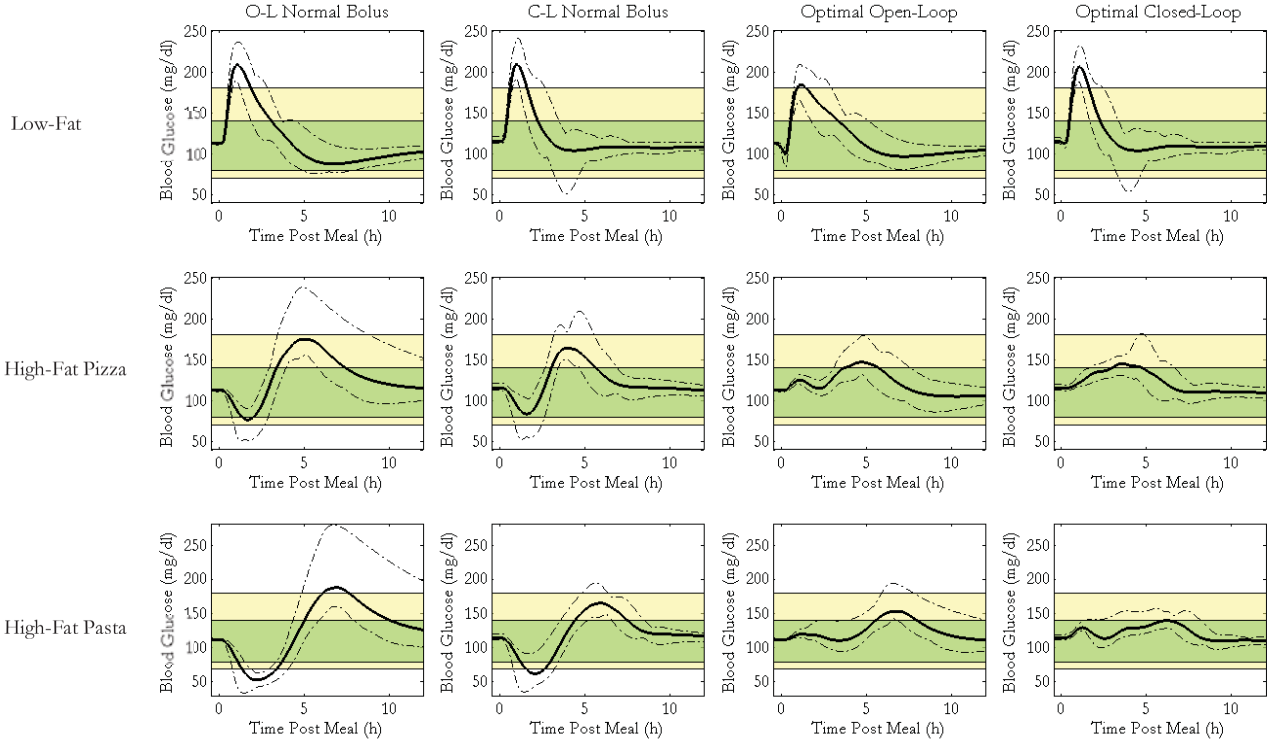

Figure B3. Comparison of insulin regimen performance for three different meal types, each comprising 100 g of carbohydrates. The solid curves represent the average blood glucose response profiles for ten *in silico* subjects and the area between the dashed lines shows the range of variability.

Lund University
Department of Automatic Control
Box 118
SE-221 00 Lund Sweden

Document name
MASTER THESIS

Date of issue
October 2013

Document Number
ISRN LUTFD2/TFRT--5928--SE

Author(s)
Asavari Srinivasan

Supervisor
Frank Doyle, Department of Chemical Engineering, University of California, Santa Barbara
Rolf Johansson, Dept. of Automatic Control, Lund University, Sweden (examiner)

Sponsoring organization

Title and subtitle

Novel Insulin Delivery Profiles for Mixed Meals in Basal-Bolus and Closed-Loop Artificial Pancreas Therapy for Type 1 Diabetes Mellitus

Abstract

Traditional basal-bolus and closed-loop artificial pancreas therapy for type 1 diabetes mellitus were studied in the present work and novel insulin delivery profiles have been identified.

Type 1 diabetes is a chronic condition resulting from autoimmune destruction of the pancreatic insulin producing β-cells. Inadequate insulin secretion prevents efficient glucose metabolism and is a serious health risk. Major available treatment modes are multiple daily injections of insulin and insulin pump therapy providing continuous subcutaneous infusion. General insulin regimens for low- and high-fat meals were studied *in silico* to improve current pump therapy for type 1 diabetes. This involved modifications of the FDA-accepted UVA/Padova metabolic simulation model for evaluations of meals with different absorption rates. Simulations of meals with varied fat content under this modified model demonstrated qualitative replications of published data. Subsequently, an insulin regimen library with optimized regimens under open- and closed-loop settings for a variety of meal compositions was constructed using the particle swarm optimization algorithm.

Calculations show that the optimal open-loop insulin delivery profiles for low-fat meals comprise a normal bolus or short square wave depending on the size of the meal. The preferred delivery pattern for large meals is a short insulin wave due to the increased risk for hypoglycemia. Interestingly, the optimal open-loop regimens for high-fat meals are typically biphasic, but can extend to multiple phases for large slow absorbing meals. Furthermore, individual *in silico* optimizations revealed that patients with high insulin sensitivity could benefit from biphasic insulin deliveries when consuming high-fat meals. Preliminary investigations of the optimal closed-loop regimens under varied fat content also display bi- or triphasic patterns for high-fat meals and are primarily influenced by the carbohydrate content in the meal.

The novel insulin delivery profiles identified in this work comprise new and unique waveforms that provide better control of postprandial glucose excursions than existing schemes. Furthermore, the novel regimens are also more or similarly robust to uncertainties in various parameter estimates with the closed-loop schemes displaying superior performance and robustness. The proposed closed-loop strategy does not rely on optimal basal therapy and is therefore a realistic approach that could have real-life applications in an artificial pancreas.

Keywords
type 1 diabetes, insulin pump therapy, insulin dosage, artificial pancreas, particle swarm optimization, biomedical control

Classification system and/or index terms (if any)

Supplementary bibliographical information

ISSN and key title
0280-5316

ISBN

Language
English

Number of pages
1-78

Recipient's notes

Security classification

http://www.control.lth.se/publications/